Retention of per- and polyfluoroalkyl substances (PFAS) in natural groundwater by soil material from a permeable reactive barrier with Colloidal Activated Carbon

Frida Lundell

Degree project/Independent project • 30 credits
Swedish University of Agricultural Sciences, SLU
Department Soil, Water and Environment
Examensarbeten / Institutionen för mark och miljö, SLU
Part number: 2025:16
Uppsala 2025

Retention of Per- and polyfluoroalkyl substances (PFAS) in natural groundwater by soil material from a permeable reactive barrier treated with Colloidal Activated Carbon

Frida Lundell

Supervisor:	**Dan Berggren Kleja, Swedish University of Agricultural sciences, department of Soil and Environment**
Assistant supervisor:	Fritjof Fagerlund, Uppsala University, department of Earth sciences
Examiner:	Jon-Petter Gustafsson, Swedish University of Agricultural Sciences, Department of Soil and Environment

Credits:	30 credits
Level:	Advanced A2E
Course title:	Master Thesis in Soil science, A2E
Course code:	EX0880
Programme/education:	Soil, Water and Environment
Course coordinating dept:	Department of Soil and Environment
Place of publication:	Uppsala
Year of publication:	2025
Series title:	Examensarbeten / Institutionen för mark och miljö, SLU
Part number:	2025:16
Copyright:	All featured images are used with permission from the copyright owner.
Keywords:	PFAS, Sorption, Colloidal Activated Carbon, Permeable reactive barrier, Groundwater, PFOS, TOP assay, In-situ remediation

Swedish University of Agricultural Sciences
Faculty of Natural Resources and Agricultural Sciences
Department Of Soil and Environment

Abstract

Per- and polyfluoroalkyl substances (PFAS) are highly persistent contaminants frequently found in the environment, including groundwater. This study investigates the sorption behavior of PFAS in colloidal activated carbon (CAC)-amended soil using batch tests with both natural and artificial groundwater. The aim was to evaluate how effectively PFAS are retained by a CAC-treated permeable reactive barrier under varying conditions, including different liquid-to-solid (L/S) ratios and water chemistries, and to assess the potential long-term performance of such barriers in in-situ remediation.

The results show that long-chain PFAS, especially PFOS and PFHpS, exhibited the strongest sorption, while short-chain compounds like PFBA showed significantly lower retention. Sorption data for natural groundwater series fit best to the Langmuir model, suggesting a finite number of sorption sites and risk of barrier saturation. The Total Oxidizable Precursor (TOP) assay also revealed precursor compounds forming PFAAs with variable sorption behavior.

Overall, the findings support CAC as a promising material for retaining long-chain PFAS in subsurface barriers, but also highlight challenges regarding short-chain mobility, precursor transformation, and long-term effectiveness.

Keywords: PFAS, Sorption, Colloidal Activated Carbon, Permeable reactive barrier, Groundwater, PFOS, TOP assay, In-situ remediation

Table of contents

List of tables: **6**

List of figures **7**

Abbreviation **8**

1. Introduction **9**

1.1 Overview of PFAS compounds and their properties 9

1.2 Applications, sources, and regulation of PFAS 10

1.3 Environmental impact 11

1.4 Sorption mechanisms 13

1.5 PFAS remediation techniques 14

2. Aim and research question **16**

3. Method **17**

3.1 Site description 17

3.2 Composition of Natural Groundwater 17

3.3 Artificial groundwater composition 19

3.4 Composition of soil 20

3.5 Batch shaking tests 22

3.5.1 Analysis of PFAS 24

3.5.2 pH measurements 24

3.6 Sorption Isotherms 25

3.6.1 Calculations 26

3.6.2 Sorption Isotherm Modelling 28

4. Results **29**

4.1 Sorption Isotherms natural groundwater 29

4.2 PFOS Sorption Isotherm in Artificial Groundwater 34

4.3 Comparison of PFOS Sorption in Natural and Artificial Groundwater Systems 35

4.4 Release of Background PFAS from Soil in the Isolated PFOS System 36

4.5 PrePFAAs 39

4.6 pH measurements 41

5. Discussion **43**

5.1 Sorption behaviour in natural groundwater 43

5.1.1 Retention of PFCAs and PFSAs in the natural groundwater system 43

5.1.2 Sorption Isotherm model fit for natural groundwater 44

5.1.3 Comparison with untreated soil 46

5.2 Sorption behaviour isolated PFOS system 47

5.2.1 Sorption Isotherm for artificial groundwater system 47

5.2.2 Comparison between artificial groundwater system and natural groundwater system....47
5.2.3 Displacement of native PFAS from soil....48
5.3 Precursor compounds....49
5.3.1 Sorption of prePFAAs to Colloidal Activated Carbon barrier....49
5.4 pH Conditions and Their Potential Influence....50
5.5 Limitations....50
5.6 Implications for In Situ Applications....51
5.7 Conclusion....51
5.8 Future recommendations....52
6. References....54
Popular science summary....57
6.1 PFAS in Soil and Water: Can Colloidal Activated Carbon Particles Help Stop the Spread?....57
Appendix 1....58

List of tables:

Table 1. Composition of natural groundwater, concentrations of cations and trace elements. 18

Table 2. Concentrations of PFAS in the groundwater before experiments (target) and concentrations after Total Oxidizable Precursor (TOP) assay. 19

Table 4. Composition of artificial groundwater, salts added to the solution in mM. Amount PFOS standard (1.35 mg/mL) (mM) added to the solution to create concentrations of 100 µ/L, 1000 µ/L PFOS artificial groundwater. ..... **Fel! Bokmärket är inte definierat.**

Table 5. Concentrations of PFAS and related compounds in the soil in µg/kg..... **Fel! Bokmärket är inte definierat.**

Table 6. Real liquid-to-solid ratios, total amount of water (mL) added to each test tube including water content from the soil, amount of soil added to each test tube, in fresh weight (g). For natural groundwater samples (1-8). ..... **Fel! Bokmärket är inte definierat.**

Table 7. Real liquid-to-solid ratios, total amount of water (mL) added to each test tube including water content from the soil, amount of soil added to each test tube, in fresh weight (g). For artificial groundwater samples (9-15). .. **Fel! Bokmärket är inte definierat.**

Table 8. Langmuir isotherm model parameters for individual PFAS compounds and the sum of 9 PFAS (Σ9 PFAS). PFOS (1) represents PFOS in the natural groundwater system). Qmax (µmol/g) represents the maximum sorption capacity, and KL (L/µmol) is the Langmuir affinity constant. P-values indicate the significance level of the parameter estimates (*p < 0.05, **p < 0.01, ***p 0.000). ..... **Fel! Bokmärket är inte definierat.**

Table 9. Partitioning coefficients (K_d) (Lkg-1) and Organic Carbon-Water Partition Coefficient (K_{OC}) (lkg-1). All values are averages of L/S ratio 4, 8, 20 and 40. The soil contains 0.152% organic carbon..... **Fel! Bokmärket är inte definierat.**

Table 10. Distribution coefficients (K_d, L/kg) for selected PFAS across the different real L/S ratios. Compounds are sorted by carbon chain length (C). * 6:2 FTS includes six fluorinated and two non-fluorinated carbon atoms.. **Fel! Bokmärket är inte definierat.**

Table 11. Partitioning coefficients (K_d) (Lkg-1) for reference samples (8A/B) and Organic Carbon-Water Partition Coefficient (K_{OC}) (lkg-1). ..... **Fel! Bokmärket är inte definierat.**

Table 12. Partitioning coefficients (K_d) (Lkg-1) for prePFBA, prePFPeA, prePFHxA and prePFHpA. ..... **Fel! Bokmärket är inte definierat.**

Table 13. pH-values for natural groundwater system (sample 1 to 9), and for artificial groundwater (sample 13 to 15). ..... **Fel! Bokmärket är inte definierat.**

List of figures

Figure 1. General classification of per- and polyfluoroalkyl compounds (OECD 2013).... 10

Figure 2. Distribution isotherms between sorbed concentration in soil (Q_e) (µmol/kg) and PFAS in aqueous phase after equilibrium (C_e) (µmol/l). 31

Figure 3. The y-axis represents the partitioning coefficient (K_d) (L/kg) and the x-axis represents carbon chain length for PFCAs (green dots) and PFSAs (blue dots). 32

Figure 4. The relationship between the equilibrium aqueous concentration (C_{eq}) in µmol/L and the sorbed concentration (C_s) in µmol/g of PFOS in batch tests. The blue dots represent samples with artificial groundwater spiked with 100 µg/L and 1000 µg/L PFOS. 35

Figure 5. The relationship between the equilibrium aqueous concentration (C_{eq}) in µmol/L and the sorbed concentration (C_s) in µmol/g of PFOS in batch tests. The blue diamond's represent samples with artificial groundwater spiked with 100 µg/L and 1000 µg/L PFOS, while the red triangles represent samples with natural groundwater with 72 µg/L PFOS. 36

Figure 6. C_{eq} of PFBA, PFPeA, PFHxA, PFOA, PFHpS and PFHxS (100 µg/L) in artificial groundwater spiked with PFOS (100µ/L). Grouped after L/S ratios. 38

Figure 7. C_{eq} of PFBA, PFPeA, PFHxA, PFOA, P37DMOA, PFHxS and PFHpS (µ/L) in artificial groundwater spiked with PFOS (1000µg/L). Grouped after L/S ratios. 38

Figure 8. Freundlich sorption isotherms for pre-PFAA compounds from the TOP assay of groundwater samples. The figures show distribution between sorbed concentration in soil (C_s) (µmol/g) and PrePFAAs in aqueous phase after equilibrium (C_{eq}) (µmol/l). Each curve represents data from multiple sampling points with varying L/S ratios. 40

Figure 9. Freundlich isotherms for pre-PFAA compounds from the TOP assay of groundwater samples plotted as log(C_s) on y-axis and log(C_{eq}) on the x-axis. The Freundlich coefficients (Kf)is displayed in the figures. 41

Abbreviation

Abbreviation	Description
AC	Activated Carbon
AER	Anion Exchange Resin
AFFF	Aqueous Film-Forming Foam
CAC	Colloidal Activated Carbon
C_{eq}	Equilibrium concentration
C_s	Solid-phase concentration
DOC	Dissolved Organic Carbon
GAC	Granular Activated Carbon
K_d	Distribution coefficient
K_L	Langmuir constant
K_{OC}	Organic carbon-normalized distribution coefficient
L/S	Liquid-to-solid ratio
PAC	Powdered Activated Carbon
PFAA	Perfluoroalkyl acid
PFAS	Per- and polyfluoroalkyl substances
PFBA	Perfluorobutanoic acid
PFCA	Perfluoroalkyl carboxylic acid
PFHpA	Perfluoroheptanoic acid
PFHxA	Perfluorohexanoic acid
PFHxS	Perfluorohexanesulfonic acid
PFNA	Perfluorononanoic acid
PFOA	Perfluorooctanoic acid
PFOS	Perfluorooctanesulfonic acid
PFPeA	Perfluoropentanoic acid
PFSA	Perfluoroalkyl sulfonic acid
POP	Persistent Organic Pollutant
prePFAA	Precursor-derived perfluoroalkyl acid
REACH	Registration, Evaluation, Authorisation and Restriction of Chemicals
TOP	Total Oxidizable Precursor (assay)
TS	Total Solids (dry weight)

1. Introduction

Per- and polyfluoroalkyl substances (PFAS are a group of highly persistent contaminants of global concern, frequently detected in soil, groundwater, and drinking water. Due to their widespread use, environmental mobility, and potential health risks, effective methods for monitoring and remediating PFAS are urgently needed. This thesis investigates the sorption behavior of PFAS, especially in the context of in-situ remediation using colloidal activated carbon (CAC) through batch shaking tests. A deeper understanding of PFAS retention mechanisms is essential to support the development of effective and sustainable remediation strategies.

1.1 Overview of PFAS compounds and their properties

Per- and polyfluoroalkyl substances (PFAS) are a group of synthetic organic compounds made up of two parts: a hydrophobic tail and a functional head group. The tail consists of a chain of carbon atoms where the hydrogen atoms are either fully or partially replaced by fluorine (F) atoms (Buck et al. 2011; Leung et al. 2023). If all hydrogen atoms along the carbon chain is replaced by fluorine, the compound is called a perfluoroalkyl substance. If only some hydrogen atoms are replaced by fluorine, it is known as a polyfluoroalkyl substance (Buck et al. 2011).

PFAS are highly persistent in the environment due to the strong and stable carbon-fluorine (C-F) bond. This bond gives PFAS high chemical and thermal stability, making them resistant to natural degradation processes (Buck et al. 2011; Leung et al. 2023). As a result, PFAS tend to accumulate in the environment over long periods of time (Leung et al. 2023).

One of the most studied groups within PFAS is perfluoroalkyl acids (PFAAs), which includes two of the most studied subgroups perfluoroalkyl sulfonic acids (PFSAs) and perfluoroalkyl carboxylic acids (PFCAs) (Buck et al. 2011) (figure 1). Among these, the most well-known and extensively researched compounds are Perfluorooctanesulfonic acid (PFOS) from the PFSA group, and Perfluorooctanoic acid (PFOA) from the PFCA group (Buck et al. 2011; Leung et al. 2023). These substances are among the oldest commercially produced PFAS and are commonly detected in environmental samples (Leung et al. 2023).

PFAS are also categorized based on the length of their carbon chain. Long-chained PFSAs are defined as having six or more carbon atoms, and long-chained PFCAs have seven or more carbon atoms (Buck et al. 2011; OECD 2013).

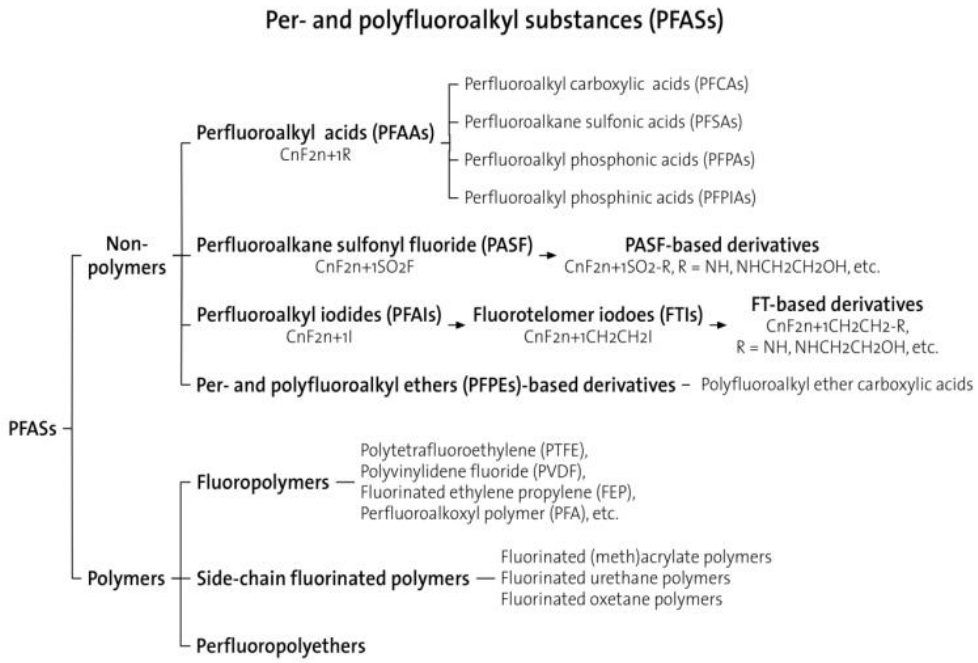

Figure 1. General classification of per- and polyfluoroalkyl compounds (OECD 2013).

Some polyfluoroalkyl substances can degrade into more persistent PFAS in the environment (OECD 2013). These precursor compounds, such as fluorotelomer-based substances and perfluoroalkane sulfonyl fluorides (PASF), contain at least one perfluoroalkyl group and can transform into stable PFAS like PFCAs and PFSAs through both biological and chemical processes (Buck et al. 2011).

However, many precursors remain unidentified in environmental samples. To detect the presence of these unknown compounds, the Total Oxidizable Precursor (TOP) assay can be applied. In this method, the concentration of PFAAs in a sample is first measured. An oxidizing agent is added to convert precursor compounds to measurable PFAAs. A second measurement of PFAAs after oxidation allows for an estimation of the total amount of precursors in the sample (i.e. prePFAAs) (Kärrman et al. 2019; Lange et al. 2024).

1.2 Applications, sources, and regulation of PFAS

To date, more than 4700 PFAS compounds have been identified (OECD 2018). These substances are entirely synthetic and do not occur naturally in the environment (Swedish Chemicals Agency 2025). Many PFAS function as surfactants due to their structure, with a hydrophobic (water repelling) tail and hydrophilic (water-attracting) head. This combination allows PFAS to reduce surface tension between liquids or within a liquid (Buck et al. 2011). Due to their

surfactant properties, as well as resistance to water, heat, and oil, PFAS have been widely used since the 1950s in a variety of consumer and industrial applications (OECD 2013; Leung et al. 2023). These include firefighting foams, food packaging, cosmetics, textiles, cookware, and household products (OECD 2013; Swedish Chemicals Agency 2025).

Airports have historically been used as military training facilities and for firefighting exercises.

Aqueous film-forming foam (AFFF), used extensively at these sites, is a well-known source of PFAS, particularly PFOS, which was commonly used due it its effectiveness in forming a film barrier between the foam and the burning liquid (Swedish Chemicals Agency 2025). The release of AFFF can cause long-distance transport, with contamination detected several kilometres from the original source (Sörengård et al. 2022). In Sweden, former fire training areas have been identified as some of the largest sources of PFAS contamination in the environment (Hansson et al. 2016). PFAS contamination of drinking water sources has been observed near several of these sites, where PFOS has been observed as the dominant PFAS compound (Ahrens et al. 2015; Koch et al. 2020; Sörengård et al. 2022; Mussabek et al. 2023).

To limit the spread of PFAS in the environment, several regulatory actions have been introduced. Sence 2009, PFOS and its salts have been listed under the Stockholm Convention on Persistent Organic Pollutants (POPs). In 2019, PFOA and its salts were added to the list. PFHxS fallowed in 2022, and in 2023 PFCAs with chain lengths of C9-C14 and their salts became restricted under the EU's REACH regulation.

From January 1st, 2026, new drinking water limits for PFAS will be enforced in Sweden, divided into two regulatory groups. The first group, known as PFAS 4, includes PFOA, PFNA, PFOS, and PFHxS, with a maximum allowable concentration of 4 ng/L. The second group, PFAS 21, encompasses the PFAS 4 compounds along with 17 additional PFAS substances, with a combined limit of 100 ng/L (Livsmedelsverket 2023).

1.3 Environmental impact

PFAS can be found in various environmental compartments including soil, water, air, and sediment, due to their high mobility and resistance to degradation (Evich et al. 2022)

Transport of PFAS occurs through several pathways. In aquatic systems, both surface water and groundwater can carry PFAS over long distances (Sörengård et al. 2022). Certain volatile PFAS (vPFAS), such as fluorotelomer alcohols

(FTOHs), can also be emitted into the atmosphere and be transported globally (Ross et al. 2018; Evich et al. 2022). A study by Kärrman et al. (2019) found elevated levels of PFAS in polar bears in Greenland, far from a known local source, indicating atmospheric transport.

Groundwater contamination by PFAS is a growing concern due to the high solubility and environmental persistence, especially compounds within the group of PFAAs. These properties can lead to the formation of plumes, which are elongated zones of contamination that move with groundwater, especially in soils or geological layers where water flows easily. This allows PFAS to spread far from their original source, possessing a major challenge for the remediation of contaminated areas (Ross et al. 2018; Evich et al. 2022).

Leaching is an important mechanism for the spread of PFAS, especially in the subsurface. When rainfall or infiltrating water comes into contact with contaminated soil, PFAS compounds can be desorbed and carried downward through the soil profile.

Due to their high mobility, short-chain PFAS, are particularly prone to leaching and can travel into deeper soil layers and aquifers (Navarro et al. 2024). Long-chain PFAS tend to bind more strongly to soil particles and organic matter, often remaining in the unsaturated soil layer above the groundwater table or accumulating in sediments (Ahrens et al. 2010; Navarro et al. 2024).

PFAS can bioaccumulate in organisms and move through food chains (Ahrens & Bundschuh 2014; Koch et al. 2020). Exposure can occur through inhalation of aerosols, ingestion of contaminated food or drinking water (OECD 2018). Koch et al. (2020) found higher PFAS concentrations in aquatic invertebrates compared to terrestrial species near a site contaminated by AFFF. Where PFOS were the most abundant PFAS found in the organisms followed by PFHxS (Koch et al. 2020). Since both PFOS and PFHxS are commonly found at sites contaminated by AFFF (Ahrens et al. 2015), it is crucial to address these pollutants due to their well-documented tendency to bioaccumulate in organisms.

Similarly, Ahrens et al. (2015) reported elevated PFAS levels in fish tissue and observed that the bioconcentration factor (BCF) increased with increasing chain length.

Drinking water is one of the human exposure pathways of PFAS.

Gyllenhammar et al. (2015) linked elevated PFAS levels in the serum of young women in Uppsala to consumption of contaminated drinking water.

1.4 Sorption mechanisms

Sorption is a general term used to describe the mechanisms that retain substances in soil, that include absorption, adsorption, and ion exchange. Where adsorption is when a chemical attaches and form chemical bonds directly on a solid surface. Absorption is when a chemical is taken up into the solid structure, and ion exchange is the exchange of one substance for another at the solid surface (Essington 2004). The term sorption is often used when the exact retention mechanism is unclear or when multiple processes may be occurring simultaneously.

The partitioning (sorption-desorption) has an important role in determining the distribution of organic compounds in the environment, influencing their mobility and transport (Kookana et al. 2023). Where sorption limits the mobility and bioavailability of an organic compound (Essington 2004).

The partitioning of a substance can be described by the partitioning/distribution coefficient (K_d), which quantifies the distribution between soil and solution (Essington 2004; Milinovic et al. 2015; Kookana et al. 2023). A high value indicates that a larger fraction of the substance is sorbed onto soil particles, making it less mobile. In contrast, low value suggests the contaminant is more likely to leach through the soil.

The organic carbon-normalized distribution coefficient (K_{OC}) is a parameter used to describe the sorption of organic compounds to soil or sediment organic matter. It is calculated by normalizing Kd to the fraction of organic carbon (f_{OC}) in the soil. A higher K_{OC} value indicates stronger sorption to organic matter, which in turn implies lower mobility of the compound in the environment (Milinovic et al. 2015).

The sorption chemistry of PFAS involves multiple mechanisms, strongly influenced by the compound's physicochemical properties, particularly the length of the perfluorinated carbon chain (Kookana et al. 2023). Sorption generally increases with chain length, as longer-chain PFAS exhibit greater hydrophobicity and a higher tendency to adsorb to soil particles (Milinovic et al. 2015; Ross et al. 2018; Gagliano et al. 2020; Sörengård et al. 2020; Liu et al. 2022; Niarchos et al. 2023; Bui et al. 2024; Sadia et al. 2024).

These longer-chain compounds interact more strongly with soil organic matter, where hydrophobic interactions become a dominant sorption mechanism (Ross et al. 2018; Kookana et al. 2023). This pattern has been consistently highlighted in previous studies, identifying hydrophobic forces as a key factor in PFAS retention in soils (Milinovic et al. 2015; Liu et al. 2022).

Under natural conditions, many PFAS compounds, particularly PFCAs and PFSAs, are predominantly anionic. This charge influences their electrostatic interactions, that is an important sorption mechanism in soils. Anionic PFAS can adsorb to charged mineral surfaces through electrostatic attraction, often mediated by their functional head groups (Ross et al. 2018; Leung et al. 2023; Bui et al. 2024). Typically, these interactions occur between the negatively charged PFAS head groups and positively charged sites on soil minerals. However, some PFAS compounds with cationic properties may also bind to negatively charged sorbent surfaces (Leung et al. 2023).

Soil solution chemistry further affects PFAS sorption. Factors such as pH, ionic strength, and the presence of polyvalent cations (e.g., Ca^{2+}, Mg^{2+}) can enhance sorption through cation bridging and strengthened electrostatic interactions. At the same time, dissolved organic carbon (DOC) may reduce PFAS retention by competing for sorption sites (Kookana et al. 2023).

1.5 PFAS remediation techniques

There are various techniques available for the remediation of PFAS. However, to effectively address the broad range of PFAS compounds, a combination of methods may be required. Different technologies are effective for different types of PFAS (Ross et al. 2018).

One common approach for PFAS remediation in soil or sediment is ex-situ treatment, which involves excavating contaminated material and treating it off-site. Thermal treatment is a frequently used method, where PFAS compounds are desorbed and possibly broken down at high temperatures, typically above 500 °C. Another method is soil stabilization, where the excavated soil is treated to immobilize PFAS and prevent them from leaching into the groundwater (Ross et al. 2018).

A more environmentally friendly approach is in-situ treatment, conducted directly at the contaminated site without the need to excavate and transport the soil. This approach reduces handling and disposal of PFAS-contaminated materials, which is a significant concern due to the risk of further spreading the contamination.

One promising in-situ technique for PFAS remediation is sorption using activated carbon (AC). Activated carbon is widely used in water treatment and is among the most studied methods for the removal of PFOS and PFOA from water (Ross et al. 2018). Sorption technologies rely on sorbent materials, such as Activated Carbon (AC) and Anion Exchange Resins (AERs), AERs remove PFAS through a combination of hydrophobic and electrostatic interactions (Ross et al. 2018; Liu et al. 2022). AC includes Powdered Activated Carbon (PAC), Granular

Activated Carbon (GAC) (Bui et al. 2024), and Colloidal Activated Carbon (CAC) (Sörengård et al. 2020, 2022). Where the pore size of the sorbent have an important part in how effective the sorbent is (Du et al. 2014).

By injecting particulate carbon, such as CAC into an aquifer, a permeable reactive barrier can be created. This barrier allows groundwater to pass through while PFAS compounds sorb to the carbon material, forming a "trap-and-treat" system for in-situ remediation (Ross et al. 2018).

However, using CAC to create a permeable barrier has some limitations. One concern is that, once the sorbent becomes saturated, it may act as a secondary source zone, potentially re-releasing PFAS into the environment. Additionally, while activated carbon is effective at removing long-chain PFAS, short-chain PFAS may pass through the barrier more easily due to their lower sorption affinity (Ross et al. 2018; Sörengård et al. 2020; Liu et al. 2022). These shorter-chain PFAS often rely more on electrostatic interactions for removal, whereas sorption of long-chain PFAS depends more on the type of sorbent and the mechanism of adsorption (Sörengård et al. 2020, 2022)

Organic matter (OM) in the soil or groundwater can also compete with PFAS for available sorption sites (Ross et al. 2018; Liu et al. 2022), as can other PFAS compounds (Niarchos et al. 2023), and inorganic ions present in the solution (Ross et al. 2018).

2. Aim and research question

The aim of this thesis is to investigate the sorption behavior of PFAS compounds in CAC-amended soil with both natural and artificial contaminated groundwater, focusing on how environmental factors such as groundwater composition and liquid-to-solid ratios influence PFAS retention in potential field-scale barrier systems.

This work is guided by the following research questions:

How does PFAS sorption differ between a natural groundwater matrix containing multiple PFAS compounds and an artificial system containing only PFOS, using the same CAC-amended soil?

How do different liquid-to-solid (L/S) ratios affect the sorption capacity of CAC-amended soil, and what implications does this have for predicting long-term PFAS retention in a CAC barrier system?

By answering these questions, the study aims to contribute to a better understanding of PFAS mobility and the practical performance of CAC-based barriers for in-situ remediation applications.

3. Method

3.1 Site description

The natural groundwater and soil used in this study were collected from a location in Örnsköldsvik, Sweden. The sampling site is located at an airport where a former fire training area is known to have used aqueous film-forming foam (AFFF). These types of firefighting foams typically contain high concentrations of perfluorooctanesulfonate (PFOS), which is often the dominant PFAS compound at such sites (Ahrens et al. 2015).

At the site, a pilot-scale remediation project is ongoing to evaluate in situ stabilization of PFAS using colloidal activated carbon (CAC). This project is a collaboration between the Swedish Geotechnical Institute (SGI) and the Geological Survey of Sweden (SGU), aiming to contribute knowledge about the method and PFAS transport in contaminated soils.

Colloidal activated carbon (CAC) is used as a sorbent due to its high surface area, providing a high sorption capacity for PFAS compounds. The CAC was injected directly into the PFAS-contaminated plume to immobilize and limit the migration of PFAS in the subsurface (SGI 2025).

3.2 Composition of Natural Groundwater

Groundwater from the study site was characterized to establish baseline conditions for the batch experiments and for preparing the artificial groundwater. The analyzed parameters included general water quality indicators (pH, temperature, conductivity, chloride, sulfate, fluoride, and DOC), major cations (e.g., Na^+, K^+, Ca^{2+}, Mg^{2+}), and trace elements (e.g., Fe, Mn, Al, Zn, As, Pb). A broad range of PFAS, including both terminal and precursor compounds, were also measured.

The full list of analyzed parameters is presented in Table 1 and 2. Concentrations of PFAS in the groundwater before experiments and concentrations after Total Oxidizable Precursor (TOP) assay is shown in Table 2. Concentrations were used for comparison with artificial groundwater and to evaluate background levels of PFAS and geochemical components.

Table 1. Composition of natural groundwater, concentrations of cations and trace elements.

Substance		Unit
pH	7	
Temperature during pH measurement	21.8	°C
Conductivity	6.00	mS/m
Chloride (Cl^-)	460	µg/L
Sulfate (SO_4^{2-})	8500	µg/L
Fluoride (F^-)	<100	µg/L
DOC	<2000	µg/L
Sodium (Na)	2200	µg/L
Potassium (K)	2700	µg/L
Calcium (Ca)	5200	µg/L
Iron (Fe)	7	µg/L
Magnesium (Mg)	580	µg/L
Manganese (Mn)	1	µg/L
Aluminium (Al)	3	µg/L
Antimony (Sb)	<0.020	µg/L
Arsenic (As)	0.04	µg/L
Barium (Ba)	18	µg/L
Lead (Pb)	<0.010	µg/L
Cadmium (Cd)	0.004	µg/L
Copper (Cu)	2	µg/L
Chromium (Cr)	<0.050	µg/L
Molybdenum (Mo)	0.1	µg/L
Nickel (Ni)	0.2	µg/L
Selenium (Se)	<0.50	µg/L
Zinc (Zn)	11	µg/L

Table 2. Concentrations of PFAS in the groundwater before experiments (target) and concentrations after Total Oxidizable Precursor (TOP) assay.

Substance	Target	TOP	Unit
PFBA	140	3800	ng/L
PFPeA	510	5100	ng/L
PFHxA	740	23000	ng/L
PFHpA	120	750	ng/L
PFOA	1600	2100	ng/L
PFNA	37	47	ng/L
PFDA	<10	<10	ng/L
PFUdA	<10	<10	ng/L
PFDoA	<10	<10	ng/L
PFTeDA	<10	<10	ng/L
HPFHpA	<10	<10	ng/L
P37DMOA	<1000	<1000	ng/L
PFBS	200	200	ng/L
PFHxS	3100	3200	ng/L
PFHpS	690	700	ng/L
PFOS	72000	82000	ng/L
PFDS	<10	<10	ng/L
4:2 FTS	<10	<10	ng/L
6:2 FTS	3400	<10	ng/L
8:2 FTS	<20	<20	ng/L
PFOSA	<10	<10	ng/L
PFTrDA	<10	<10	ng/L
PFDoS	<10	<10	ng/L
PFNS	<10	<10	ng/L
PFPeS	380	390	ng/L

3.3 Artificial groundwater composition

Artificial groundwater was prepared to mimic the ionic composition of the natural groundwater while isolating the behaviour of PFOS as a single compound. The solution contained Milli-Q water and selected salts ($NaHCO_3$, KCl, $CaSO_4$, and $MgCl_2$) added in millimolar concentrations (Table 3) to reflect natural groundwater conditions. Two concentrations of PFOS, 100 µg/L and 1000 µg/L, were created by spiking the solution with a PFOS standard with a purity of ≥98.0% (1.35 mg/mL). Final PFOS concentrations were achieved by adding 0.00017 mM and 0.0020 mM of the standard to 1000 mL of the salt solution, respectively.

The artificial groundwater was used in a parallel set of batch experiments to assess PFOS sorption in the absence of other PFAS compounds and potential competitive effects.

Table 3. Composition of artificial groundwater, salts added to the solution in mM. PFOS standard (1.35 mg/mL) (mM) was added to the solution to create concentrations of 100 µ/L, 1000 µ/L PFOS artificial groundwater.

Salt	mM
NaHCO3	0.07
KCl	0.07
CaSO4	0.09
MgCl2	0.02
PFOS 100 µ/L (1.35 mg/mL)	0.00017
PFOS 1000 µ/L (1.35 mg/mL)	0.0020

3.4 Composition of soil

The soil used in the batch shaking tests is a sandy soil collected from Örnsköldsvik Airport at a depth of 4–5 meters. It was analyzed for a wide range of PFAS, including both linear and branched isomers, fluorotelomer substances, and total carbon content. The total PFAS concentration (∑PFAS) in the soil was found to be 10.69 µg/kg, of which 0.77 µg/kg consisted of perfluoroalkyl carboxylic acids (PFCAs), 7.366 µg/kg of perfluoroalkyl sulfonic acids (PFSAs), and 2.55 µg/kg of precursor compounds. These values represent the baseline contamination levels of the tested material and are detailed in Table 4. The fraction of organic carbon (f_{OC}) was measured at 0.152%, while the total carbon (TC), including both organic and inorganic carbon, was 0.2%.

Table 4. Concentrations of PFAS and related compounds in the soil in µg/kg.

Compound	Concentration (µg/kg)
Depth (m)	4–5
PFBA	<0.20
PFPeA	<0.060
PFHxA	<0.060
PFHpA	<0.060
PFOA	<0.060
PFNA	<0.060
PFDA	<0.20
PFUdA	<0.20
PFDoA	<0.20
PFTrDA	<0.20
PFBS	<0.060
PFPeS	<0.20
PFHxS	0.068
PFHpS	<0.060
PFOS	1.9
PFNS	<0.40
PFDS	<0.060
PFUnDS	<2.0
PFDoS	<2.0
PFTrDS	<2.0
4:2 FTS	<0.060
6:2 FTS	<0.060
8:2 FTS	<0.20
10:2 FTS	<1.0
PFOSA	<0.20
MeFOSA	<0.060
EtFOSA	<0.40
FOSAA	<0.20
MeFOSAA	<0.060
EtFOSAA	<0.20
MeFOSE	<0.060
EtFOSE	<0.20
6:2 FTAB	<2.0
PFOA branched	<0.060
PFOA linear	<0.060
PFNA branched	<0.060
PFNA linear	<0.060
PFHxS branched	<0.060
PFHxS linear	0.068
PFOS branched	0.51
PFOS linear	1.4
PFOSA branched	<0.20

PFOSA linear	<0.20
Total carbon	0.2
TIC (Total Inorganic Carbon)	<0.1

3.5 Batch shaking tests

Batch equilibrium tests were conducted to evaluate the sorption of PFAS to a permeable barrier of colloidal activated carbon (CAC) under varying liquid-to-solid (L/S) ratios. This method quantifies the partitioning of PFAS from a solid matrix to an aqueous phase by mixing soil with water, agitating the mixture until equilibrium is reached, and analyzing the liquid phase for PFAS concentrations (Navarro et al. 2024).

The soil used was a field-moist sandy material collected from the CAC barrier at Örnsköldsvik Airport. The organic carbon fraction (f_{oc}) was 0.152%. Natural groundwater from the same site, containing approximately 84,000 ng/L of ΣPFAS, served as the leaching solution. To minimize contamination, all equipment was rinsed three times with methanol before use.

A range of liquid-to-solid (L/S) ratios from 1 to 80 was selected based on preliminary K_d estimates, with the aim of capturing a broad spectrum of water–soil interaction scenarios. Lower L/S ratios represent conditions with low amounts of added PFAS relative to the amount of soil present, since added PFAS mainly originated from the added water. This approach allowed for the assessment of PFAS retention across varying degrees of leaching potential. All tests were prepared in 110 mL polypropylene tubes with a target solution volume of 80 mL, and each test was conducted in duplicate (e.g., 1A/1B). Two reference samples (Ref 1 and Ref 2), prepared with unamended soil from the same site at an L/S ratio of 10, were included to assess background sorption capacity.

To determine the soil's moisture content, a sample was dried at 105 °C for 42 hours. The measured water content (18.03%) was used to correct the L/S ratios and ensure accurate dosing of soil and solution in each tube. The actual soil and water amounts used in each replicate are presented in Table 5 and 6.

The samples were agitated for six days using an overhead shaker to reach equilibrium. After shaking, the suspensions were centrifuged at 3000 rpm for 20 minutes. The supernatants were then diluted threefold with Milli-Q water to meet volume requirements for PFAS and TOP analysis.

In addition to the natural groundwater tests, batch experiments were performed using artificial groundwater spiked with PFOS to isolate its sorption behavior without interference from other PFAS. Two PFOS concentrations were tested, 100 µg/L and 1000 µg/L, across selected L/S ratios (1, 8, 20, 40 for 100 µg/L and 8, 20, 80 for 1000 µg/L). The same soil and procedure were used as in the natural groundwater tests. Actual amounts of soil and spiked solution for each test are shown in Table 5.

Table 5. Real liquid-to-solid ratios, total amount of water (mL) added to each test tube including water content from the soil, amount of soil added to each test tube, in fresh weight (g). For natural groundwater samples (1-8).

Sample	L/S	Soil DW (g)	Volume water (mL)
1A	1.00	65.6	80.1
1B	1.00	65.8	80.1
2A	3.96	16.6	80.0
2B	3.98	16.5	80.1
3A	8.22	8.20	82.4
3B	8.22	8.20	82.4
4A	9.94	6.78	82.2
4B	10.1	6.66	82.2
5A	20.5	3.31	82.7
5B	20.6	3.28	82.2
6A	41.0	1.65	82.2
6B	39.1	1.72	82.2
7A	81.6	0.83	82.3
7B	84.2	0.83	84.8
8A (ref)	9.98	6.58	80.1
8B (ref)	9.99	6.57	80.0

Table 6. Real liquid-to-solid ratios, total amount of water (mL) added to each test tube including water content from the soil, amount of soil added to each test tube, in fresh weight (g). For artificial groundwater samples (9-15).

Sample	L/S	Soil DW (g)	Total amount of water (mL)
9A	1	65.7	82.7
9B	1	65.8	82.4
10A	12	8.20	82.4
10B	12	8.20	82.3
11A	29	3.28	82.3
11B	28	3.30	82.3
12A	57	1.66	82.2
12B	57	1.65	82.3
13A	12	8.20	82.3
13B	11	8.20	82.2
14A	29	3.30	82.5
14B	29	3.31	82.2
15A	113	0.836	82.2
15B	114	0.828	82.2

3.5.1 Analysis of PFAS

Two analyses were performed, target PFAS32 and Total Oxidizable Precursor (TOP) assay. The PFAS were quantified using targeted analysis, which focused on 32 individual PFAS. This approach involves the use of liquid chromatography coupled with tandem mass spectrometry (LC-MS/MS), allowing for the sensitive and selective detection of known PFAS compounds based on predefined standards. By targeting a specific list of analytes, this method provides concentration data for individual PFAS species. The TOP assay is an analytical technique designed to identify and quantify oxidizable PFAS precursors. In this method, samples are treated with a strong oxidizing agent to convert precursor compounds into stable perfluoroalkyl acids (PFAAs). These transformation products are subsequently measured using conventional target analysis methods (Eurofins Scientific n.d.).

3.5.2 pH measurements

To assess the acidity of the samples, measurements were performed using a calibrated pH meter immediately after centrifugation and removal of the supernatant for the samples sent to Eurofins for analysis. Each sample was stirred

for approximately 10 seconds prior to measurement, and the pH value was recorded once it had stabilized.

3.6 Sorption Isotherms

Adsorption isotherms are commonly used to describe how a substance interacts with a sorbent material under equilibrium conditions. They are tools in understanding sorption processes, as they allow for a quantitative assessment of how much of a contaminant remains dissolved in the aqueous phase at equilibrium ($C_{eq)}$, and how much has been adsorbed to the solid material (C_s), at a constant temperature (hence isotherm) (Essington 2004).

In this study, two widely used isotherm models were applied to describe the adsorption behavior of PFAS compounds: the Langmuir and Freundlich isotherms.

The Langmuir isotherm assumes that sorption occurs at specific, identical sites on a homogenous surface, leading to the formation of a single molecular layer. This model also assumes that once a site is occupied, no further adsorption can occur there. It is described by the following equation:

1) $$q_e = \frac{q_{max} \cdot K_L \cdot C_{eq}}{(1+K_L \cdot C_{eq})}$$

Equation 1, q_e is the amount of contaminant adsorbed per unit weight of adsorbent (at equilibrium), q_{max} is the maximum adsorption capacity, K_L is the adsorption constant, related to the binding affinity and C_{eq} is the equilibrium concentration in the aqueous phase (Essington 2004).

In contrast, the Freundlich isotherm is an empirical model that describes adsorption on heterogenous surfaces and does not assume maximum capacity. It accounts for the fact that adsorption may occur at sites with varying energies. The general form of the Freundlich equation is:

2) $$q = K_F \cdot C_{eq}^N$$

Equation 2, KF is a constant indicating the relative adsorption capacity and N is a constant reflecting the intensity or heterogeneity of the adsorption process. To facilitate linear regression, the Freundlich model is often expressed in logarithmic form:

3) $\log q = logK_F + N\ logC_{eq}$

When plotted with log (C_{eq}) on the x-axis and log (C_s) on the y-axis, a straight line indicates that the model fits the data well. In this linear form, N is the slope of the line and log KF is the y-intercept (Essington 2004).

The linear sorption isotherm is one of the simplest models used to describe the relationship between the amount of a substance sorbed to a solid phase (Q_e) and its concentration in the liquid phase at equilibrium (C_e). It assumes that sorption increases proportionally with concentration and is mathematically expressed as:

4) $Q_e = K_d \cdot C_e$

where K_d is the distribution coefficient. This model corresponds to a Freundlich isotherm with the exponent n=1, meaning that the sorption sites are homogeneous and have equal affinity for the sorbate across the tested concentration range. Linear isotherms are typically applicable when sorption occurs at low concentrations, where the available sorption sites are far from saturated. This condition is often relevant in environmental systems, such as groundwater, where contaminant levels are generally low. The simplicity of the linear model makes it useful for comparing sorption behavior and for use in transport modeling, though it may not capture nonlinearity at higher concentrations (Essington 2004).

3.6.1 Calculations

The partitioning coefficient (K_d) is a measure of how much a substance partitions between the solid and liquid phase, was calculated according to equation 4. Where C_s is the sorption to soil and calculated according to equation 1. C_{eq} is the concentration of PFAS in the aqueous phase after reaching equilibrium.

5) $K_d = \frac{C_s}{C_{eq}}$

Sorption to soil was calculated according to:

6) $C_S = \frac{(C_{in} \cdot V_{in} - C_{eq} \cdot V_{tot})}{m_{soil}}$

where C_s is the sorption of PFAS to the soil, C_{in} is the ingoing concentration in the groundwater and in the artificial groundwater used in the PFOS isolated

system. C_{eq} is the concentration of PFAS in the aqueous phase after reaching equilibrium, V_{in} is the volume of the water added to the test tubes, V_{tot} is the total volume including water content in the soil and m_{soil} is the amount of dry weight soil added to the test tubes.

Sorption of oxidizable PFAS precursors to soil was calculated using equation 6. The concentration of sorbed compounds (C_s, in µmol/g) was determined by measuring the increase in perfluoroalkyl acids (PFAAs) before and after the TOP assay, referred to as prePFAA. The difference in prePFAA concentration between the initial (before equilibrium) and final (after equilibrium) timepoints reflects the amount of precursor adsorbed to the soil. The calculation is based on the following equation:

$$7) \quad C_s(TOP) = \frac{(prePFAA_{initial} \cdot V_{initial}) - (prePFAA_{equlibrium} \cdot V_{equlibrium}}{msoil}$$

where C_s is the concentration of precursor sorbed to soil (µmol/g), prePFAA is the concentration of PFAA formed after the TOP assay minus concentration before TOP assay (µmol/L). $V_{initial}$ is the aqueous volume before equilibrium (L). $V_{equilibrium}$ is the corrected aqueous volume after equilibrium, accounting for water retained in the soil (L), and m_{soil} is the mass of soil (g).

To further evaluate the sorption behavior, the distribution coefficient after the TOP assay K_d (TOP) was calculated as:

$$8) \quad K_d(TOP) = \frac{Cs\ TOP}{Ceq\ TOP}$$

This coefficient describes the partitioning of oxidizable precursors between the solid and aqueous phases following oxidation and provides a basis for comparing sorption tendencies among different unknown precursor compounds.

The percentage of PFAS mass desorbed from the soil into the aqueous phase after shaking was calculated using equation:

$$9) \quad Desorption\ (\%) = \left(\frac{M_{water}}{M_{soil}}\right) \cdot 100$$

M_{water} is the mass of PFAS measured in the aqueous phase after shaking (ng). M_{soil} is the estimated initial PFAS mass in the soil before shaking (ng).

3.6.2 Sorption Isotherm Modelling

The Langmuir isotherm model was fitted to experimental data using R Studio, which allowed for nonlinear regression and parameter estimation. The Freundlich model parameters were calculated using Excel through linear regression of the logarithmic form of the Freundlich equation. All values below Limit of detection (LOD) were not used to compile these results.

4. Results

The following results are based on experimental data derived from batch shaking tests, as well as analytical results provided in Appendix 1. This appendix contains the raw data files that form the foundation for all data processing, model fitting, and interpretation presented in this section.

4.1 Sorption Isotherms natural groundwater

The Freundlich isotherm model was applied to evaluate the adsorption behavior of the individual PFAS compounds. Visual inspection of the fitted curves showed that the model did not adequately represent the adsorption pattern for certain substances (e.g., PFHxA, PFHpS, 6:2 FTS, 6:2 FTS, PFOA and PFOS both in natural groundwater and isolated system). The Freundlich model did not capture the plateauing or non-linear curvature observed in the data, suggesting that its assumption of multilayer adsorption on heterogenous surface may not be appropriate for these compounds.

The Langmuir isotherm model was applied instead, which assumes monolayer adsorption on a surface with maximum binding capacity. For the PFAS compounds where the Freundlich model did not describe the data well, the Langmuir model was applied to produce a more representative fit.

Langmuir isotherm model parameters were estimated for individual PFAS compounds and for the sum of nine PFAS (Table 7). Q_{max} values ranged from 0.00000533 µmol/g (PFHpA) to 0.00450 µmol/g (Σ9 PFAS). The highest Q_{max} values were observed for PFOS (0.00390 µmol/g) and Σ9 PFAS (0.00450 µmol/g). KL values ranged from 140 L/µmol (PFPeA) to 69,500 L/µmol (PFPeS). The P-values for Q_{max} were statistically significant ($p < 0.05$) for most compounds except PFHpA and PFPeA. For KL, significant p-values ($p < 0.05$) were found for PFHpS, PFOA, PFOS (1), and Σ9 PFAS. A lack of statistical significance (i.e., no asterisk) indicates that the model could not confidently estimate that parameter based on the available data, which may reflect high variability or weak sorption.

P-values are indicated in the table as follows: ***$p < 0.001$, **$p < 0.01$, *$p < 0.05$, no asterisk = not significant ($p \geq 0.05$).

*Table 7. Langmuir isotherm model parameters for individual PFAS compounds and the sum of 9 PFAS (Σ9 PFAS). PFOS (1) represents PFOS in the natural groundwater system). Q_{max} (µmol/g) represents the maximum sorption capacity, and K_L (L/µmol) is the Langmuir affinity constant. P-values indicate the significance level of the parameter estimates (*p < 0.05, **p < 0.01, ***p 0.000).*

Compound	Q_{max}	K_L	P-value q_{max}	P-value K_L
PFHxA	0.0000113	23 700	0.00234**	0.690
PFHpS	0.0000397	17 100	0.000000903***	0.00322
PFOA	0.0000669	6050	0.00000101***	0.00763**
6:2 FTS	0.000149	4060	0.00014***	0.107
PFOS (1)	0.00390	209	0.00007438394***	0.033
PFHxS	0.000105	4890	0.000121***	0.138
PFHpA	0.00000533	22 700	0.804	0.873
PFPeA	0.0000453	140	0.849	0.872
PFPeS	0.00000875	69 500	0.0224	0.726
Σ_9 PFAS	0.00450	102	0.0000148***	0.0138*

Figure 2 shows Langmuir sorption isotherms for nine individual PFAS compounds (PFHxA, PFHpA, PFOA, PFHpS, PFHxS, PFPeA, PFPeS, PFOS, and 6:2 FTS) as well as the summed concentration of these compounds (Σ_9 PFAS). Each plot displays the equilibrium concentration in solution (C_e, µmol/L) on the x-axis and the corresponding amount adsorbed per gram of adsorbent (Q_e, µmol/kg) on the y-axis. Blue points represent experimental data, and red curves represent model fits.

In general, the plot shows an increase in Q_e with increasing C_e for all compounds. In several cases, such as PFOS, PFHpS, and PFPeS, the curve rises quickly and then levels off, indicating a saturation trend in adsorption. Other compounds, such as PFHxA and PFHpA, show more scattered data and a less distinct curve shape.

The Σ_9 PFAS plot, which summarizes total adsorption, shows a rise in Q_e with increasing C_e and a levelling trend. All models fit with a non-linear pattern.

No outliers or negative Q_e values are visible in the plots. The data points vary in density across compounds, with some compounds having more replicates than others.

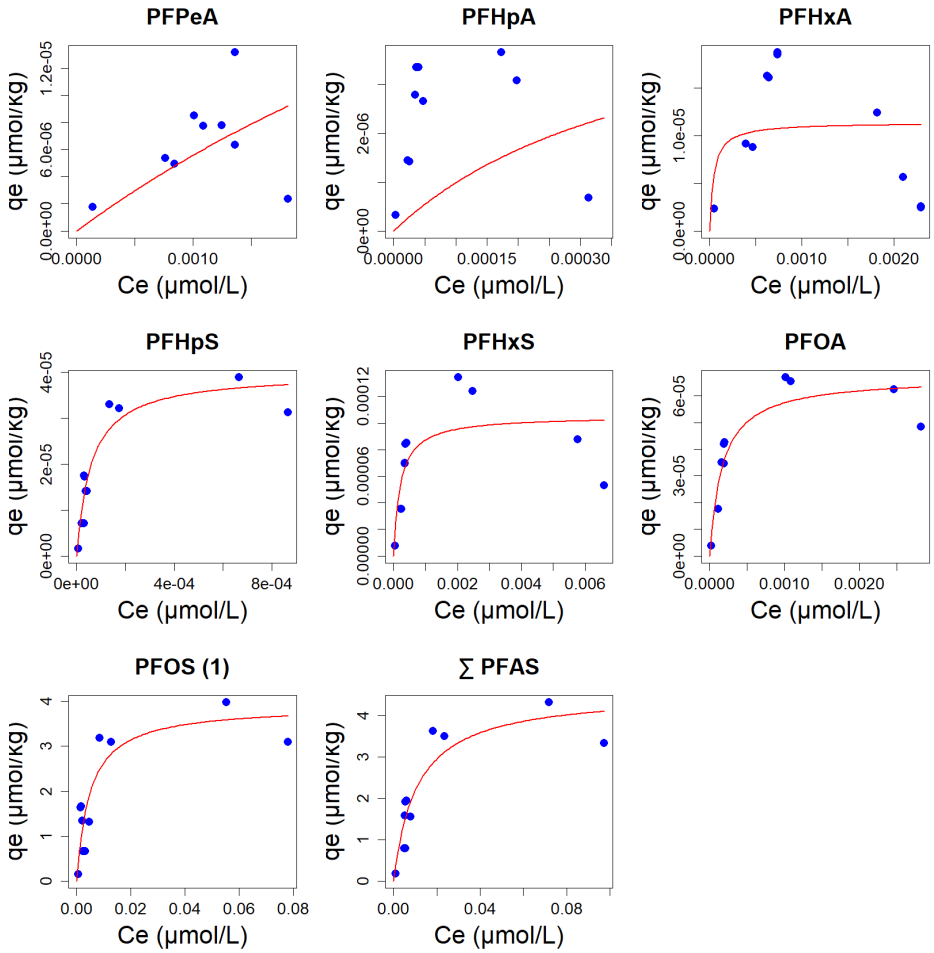

Figure 2. Distribution isotherms between sorbed concentration in soil (Q_e) (µmol/kg) and PFAS in aqueous phase after equilibrium (C_e) (µmol/L).

The average K_d, Langmuir affinity constant (K_L), and carbon-water partitioning coefficient (K_{OC}) values were summarized for each PFAS compound in the natural groundwater series (Table 8). The averages are based on data from L/S ratios 4, 8, 20, and 40, which represent the linear portion of the isotherm. Sample 1 was excluded due to only one sample being analyzed, and sample 7A showed extreme values and, thus, 7A and 7B were excluded from the average calculations.

These values represent overall sorption behavior across the tested L/S ratios. For comparative purposes, K_d values for each L/S ratio are presented separately in Table 9. Among the PFAS compounds, PFOS had the highest K_d value (402 L/kg), while PFPeA showed the lowest (6.5 L/kg). Similarly, 6:2 FTS exhibited the highest average log K_{OC} value (6.00), and PFPeA the lowest (3.62).

Standard deviations (SD) were calculated using the sample standard deviation function (STDEV.S), which estimates variability within the sample set. The SD values vary substantially between compounds and indicate differences in sorption

behaviour across replicates and L/S ratios. In general, higher SD values were observed for compounds with higher average sorption (e.g., PFOS and PFHpS), reflecting larger variation between sample replicates, likely due to sensitivity to experimental conditions or spatial heterogeneity in the CAC-amended soil.

Table 8. Partitioning coefficients (K_d) (L/kg) and Organic Carbon-Water Partition Coefficient (K_{OC}) (L/kg). All values are averages of L/S ratio 4, 8, 20 and 40. The soil contains 0.152% organic carbon.

Compound	Group	Chain length	K_d (L/kg)	K_{OC} (L/kg)	log K_{OC}	SD (K_d)	SD (K_{OC})
PFPeA	PFCA	C5	6.5	4 210	3.62	1.12	640
PFHxA	PFCA	C6	19.84	10 200	4.01	9.89	7 740
PFHpA	PFCA	C7	60.5	31 100	4.49	30.8	23 500
PFOA	PFCA	C8	167	87 900	4.94	70.6	57 500
PFPeS	PFSA	C5	66.6	45 100	4.65	36.6	29 700
PFHxS	PFSA	C6	163	84 500	4.93	70.4	59 500
PFHpS	PFSA	C7	367	234 000	5.29	147	121 000
PFOS	PFSA	C8	402	193 000	5.46	257	270 000
6:2 FTS	FTS	C8 (6:2)	190	990 000	6.00	95.4	1 960 000

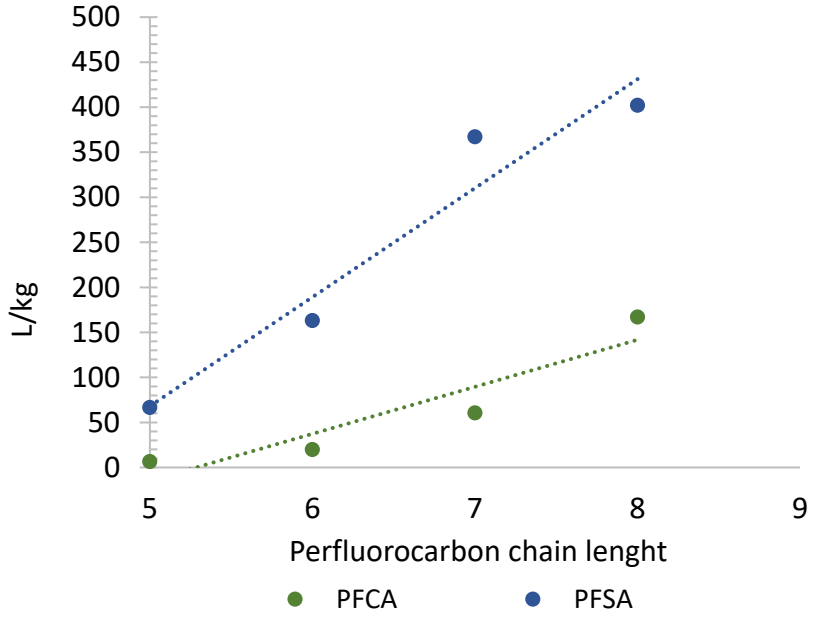

Figure 3. The y-axis represents the partitioning coefficient (K_d) (L/kg) and the x-axis represents carbon chain length for PFCAs (green dots) and PFSAs (blue dots).

Table 9 shows average partitioning coefficient (K_d) values for samples 2 to 5, with real L/S ratios 4 to 40 as previously mentioned. Sample 1 was excluded since only one sample was analyzed, as previously mentioned, and sample 7 was excluded due to extreme values on sample 7A.

PFSAs had overall higher average K_d values than PFCAs across the different L/S ratios (Figure 3). PFOS had the highest K_d value (1 130 at L/S 10). At L/S 4 and 8 respectively, PFHpS had higher K_d values than PFOS (295, 316). Lowest K_d values were observed for PFBA for all L/S ratios.

The reference soil samples (8A/B) are shown in Table 10. They have L/S of 10. Due to negative values, K_d could only be determined for PFBA, PFOA, and PFHpS. The K_d values range between 0.120 (PFOA, sample 8B) and 2.14 (PFBA, sample 8B). The K_{OC} values ranged between 80.4 (PFOA, sample 8B) and 1 410 (PFBA, sample 8B).

*Table 9. Distribution coefficients (K_d, L/kg) for selected PFAS across the different real L/S ratios. Compounds are sorted by carbon chain length (C). * 6:2 FTS includes six fluorinated and two non-fluorinated carbon atoms.*

Compound	Group	C	L/S 4	L/S 8	L/S 10	L/S 20	L/S 40
PFBA	PFCA	C4	1.36	0.91	1.67	5.59	4.32
PFPeA	PFCA	C5	6.47	7.73	5.45	5.47	13.6
PFHxA	PFCA	C6	21.1	24.3	25.3	4.76	1.1
PFHpA	PFCA	C7	60.1	72.6	87.8	18.3	2.18
PFOA	PFCA	C8	162	191	220	63.1	21.2
PFNA	PFCA	C9	183	169	347	–	–
PFBS	PFSA	C4	26.2	32.1	33.7	10.2	2.56
PFPeS	PFSA	C5	86.1	102	101	29.6	12.1
PFHxS	PFSA	C6	152	175	220	58.3	11.6
PFHpS	PFSA	C7	294	316	547	216	47.1
PFOS	PFSA	C8	250	253	1130	313	55.9
6:2 FTS	FTS	C8*	204	232	367	113	24.5

Table 10. Partitioning coefficients (K_d) (L/kg) for reference samples (8A/B) and Organic Carbon-Water Partition Coefficient (K_{OC}) (L/kg).

K_d	K_d PFBA	K_d PFOA	K_d PFHpS	K_{OC} PFBA	K_{OC} PFOA	K_{OC} PFHpS
8A	1.13	0.360	0.360	743	236	234
8B	2.14	0.120	0.940	1410	80.0	620

4.2 PFOS Sorption Isotherm in Artificial Groundwater

Figure 4 illustrates the relationship between the equilibrium concentration of PFOS in solution (C_{eq}, μmol/L) and the sorbed concentration on the solid phase (C_s, μmol/kg). The data points represent measurements from the batch tests, showing how PFOS partitions between the aqueous and solid phases at equilibrium.

In the artificial groundwater system, the linear regression equation fitted to the data is: $C_s=0.2637 \cdot C_{eq}+0.0008$, with a coefficient of determination $R^2=0.924$. This high R^2 value indicates that the model provides a good fit to the experimental data. The slope of the line (0.264 L/g) represents the distribution coefficient (K_d) in units of L/g. When converted to more conventional units, this corresponds to a K_d value of 264 L/kg.

The figure provides a visual overview of PFOS sorption behavior, highlighting the range and distribution of concentrations observed in the experiments.
The group with an initial concentration of 100 μg/L (samples 9–12) shows C_{eq} values between 0.00084 and 0.024 μmol/L, and C_s values from 0.00022 to 0.0085 μmol/kg. In the 1000 μg/L PFOS group (sample 13), C_{eq} values range from 0.060 to 0.072 μmol/L, and C_s values range from 0.005 to 0.025 μmol/kg.

The lowest C_{eq} values were observed in samples 9A/B, while the highest were found in sample 12A. Correspondingly, the lowest C_s values were observed in samples 9A/B, with the highest C_s values in sample 12B. Samples with anomalous or invalid data (e.g., extreme values or negative sorbed concentrations) were excluded from the analysis. Specifically, samples 14A and 14B were excluded due to a negative C_s value observed in sample 14B. Similarly, samples 15A and 15B were excluded from the analysis due to negative values in both replicates.

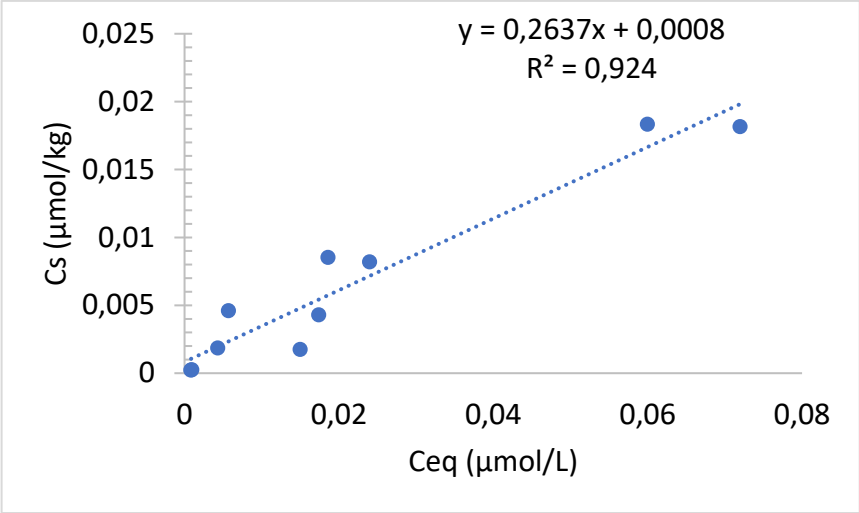

Figure 4. The relationship between the equilibrium aqueous concentration (C_{eq}) in µmol/L and the sorbed concentration (C_s) in µmol/g of PFOS in batch tests. The blue dots represent samples with artificial groundwater spiked with 100 µg/L and 1000 µg/L PFOS.

4.3 Comparison of PFOS Sorption in Natural and Artificial Groundwater Systems

Figure 5 illustrates the relationship between the equilibrium concentration of PFOS in solution (C_{eq}, µmol/L) and the sorbed concentration on the solid phase (C_s, µmol/kg) for both natural groundwater samples (red triangles) and artificial groundwater samples (blue diamonds).

In the natural groundwater samples, C_{eq} values ranged from 0.00050 µmol/L (sample 1A) to 0.078 µmol/L (sample 6A). Correspondingly, C_s values varied from 0.14 µmol/kg (sample 1A) to 4.0 µmol/kg (sample 6B). The lowest C_{eq} and C_s values were observed in sample 1A, while the highest C_{eq} occurred in sample 6A, and the highest C_s values were found in samples 5A/B and 6B. Sample 7A and 7B were excluded from the analysis due to 7A being identified as an outlier. The sorption data for natural groundwater showed an initial linear trend at lower C_{eq} values but began to level off at higher concentrations, suggesting a Langmuir-type behaviour indicative of sorption site saturation.

In contrast, the artificial groundwater samples exhibited a strong linear trend across the tested concentration range, as indicated by a high R^2 value of 0.962 for the fitted linear regression. After exclusion of samples 14A/B and 15A/B due to negative or invalid values, the calculated K_d for PFOS in this system was 264 L/kg. This linear trend indicates that within the studied range, the sorption sites were not saturated, allowing for a proportional increase in C_s with C_{eq}.

In comparison, the natural groundwater system yielded a higher K_d of 402 L/kg, reflecting stronger overall sorption under those conditions. However, this system also showed evidence of a saturation threshold at the highest L/S ratios in only two samples, limiting the certainty of this observation. Therefore, while Langmuir-like behaviour is suggested, the dataset is not sufficient to confidently confirm a definitive saturation trend.

This comparison highlights the contrasting sorption behaviours of PFOS under simplified and more complex aqueous chemistries. The artificial groundwater system, free from competing PFAS and with controlled ionic composition, supports a linear sorption model. Meanwhile, the natural groundwater system exhibits signs of nonlinear sorption.

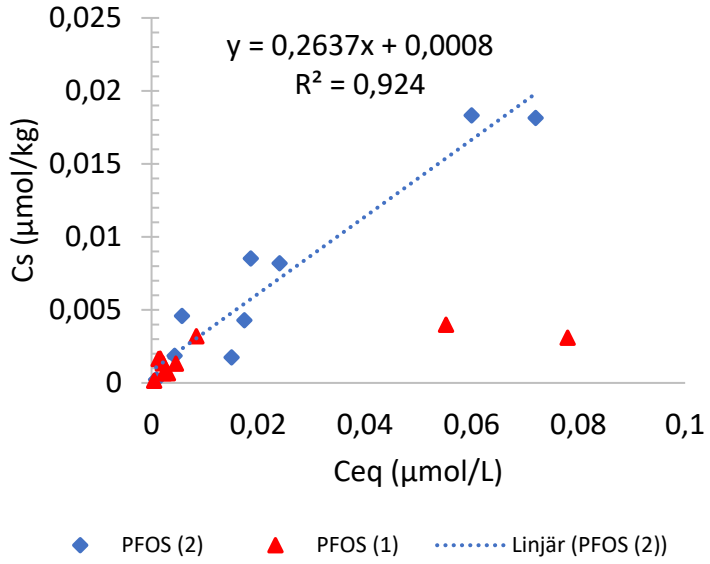

Figure 5. The relationship between the equilibrium aqueous concentration (C_{eq}) in µmol/L and the sorbed concentration (C_s) in µmol/kg of PFOS in batch tests. The blue diamond's represent samples with artificial groundwater spiked with 100 µg/L and 1000 µg/L PFOS, while the red triangles represent samples with natural groundwater with 72 µg/L PFOS.

4.4 Release of Background PFAS from Soil in the Isolated PFOS System

The artificial groundwater was spiked with PFOS standard. After reaching equilibrium elevated concentrations of additional PFAS, those not intentionally added were detected in the aqueous phase. The highest concentrations among those non-added PFAS were observed for PFHpS in both PFOS solutions (100µg/L and 1000µg/L) (Figure 6 and 7).

Detected concentrations ranged from 9.90 ng/L (L/S 1, initial PFOS concentration 100 ng/L) to 21600 ng/L (L/S 80, initial PFOS concentration 1000 ng/L).

In the 100 ng/L PFOS system, the highest concentration was detected for PFHpS (140 ng/L), followed by PFPeA (146 ng/L), PFBA (96 ng/L), PFHxA (53 ng/L), PFHpA (33 ng/L) and PFOA (14 ng/L) (Figure 6).

In the 1000 ng/L PFOS system, PFHpS again showed the highest average concentration (15 400 ng/L), followed by PFPeA (1870 ng/L), P37DMOA (1 500 ng/L), PFBA (1 100 ng/L), PFHxA (1 050 ng/L), PFHpA (1 000 ng/L), PFHxS (447 ng/L), and PFOA (390 ng/L) (Figure 7).

The percentage of PFAS mass desorbed from the soil into the aqueous phase after shaking was calculated for each compound and sample. The calculation was based on the estimated initial mass of PFAS in the soil and the measured mass in the water phase after shaking (see appendix 1).

Some samples showed desorption values exceeding 100%, indicating that the amount detected in the aqueous phase was greater than the initially estimated amount present in the soil. This suggests that part of the detected PFAS likely originated from the PFOS standard used in the spiking solution, which was specified as ≤98% pure. Therefore, it is likely that the release of PFAS into the aqueous phase after batch shaking was partly due to impurities in the standard rather than exclusively from desorption from the soil matrix.

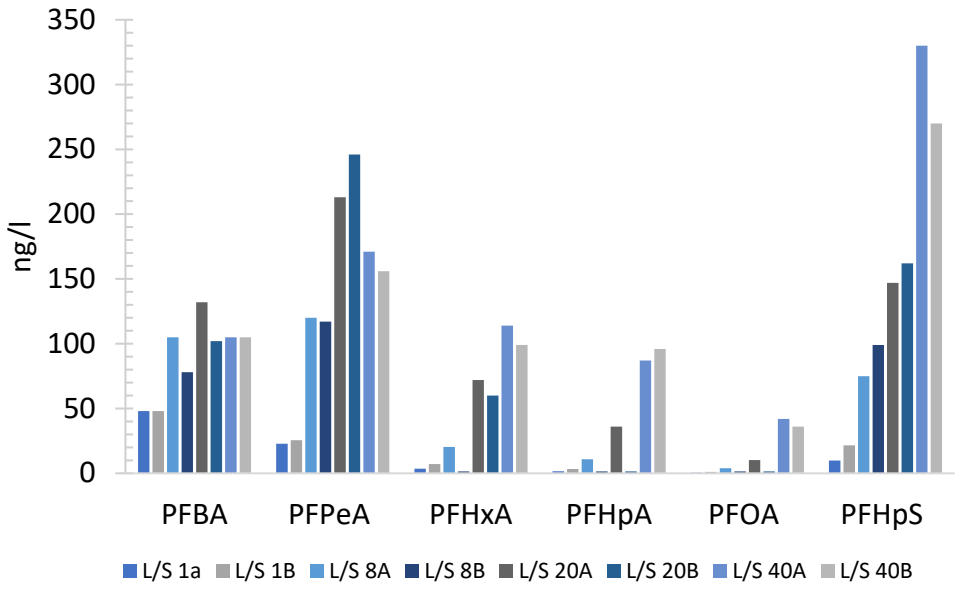

Figure 6. C_{eq} of PFBA, PFPeA, PFHxA, PFOA, PFHpS and PFHxS (100 µg/L) in artificial groundwater spiked with PFOS (100µ/L). Grouped after L/S ratios.

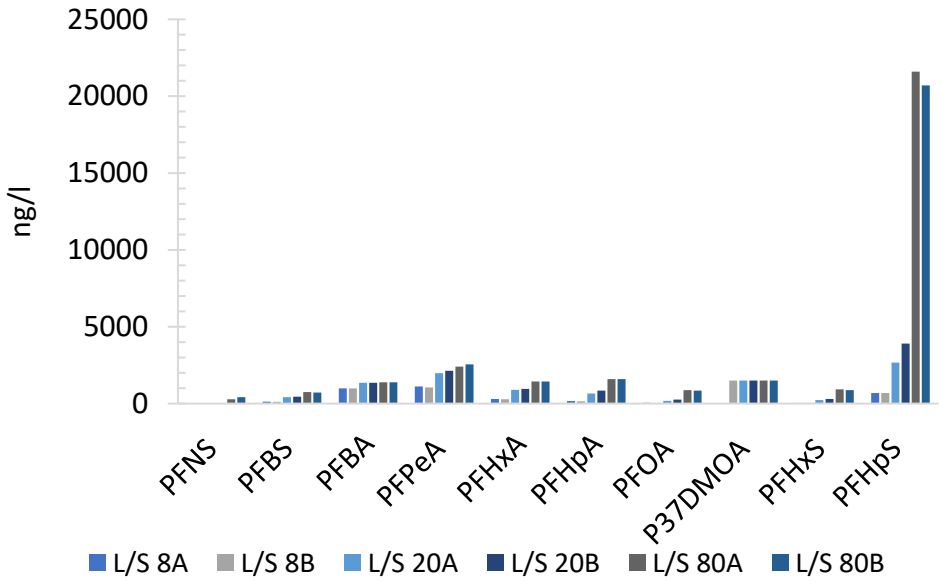

Figure 7. C_{eq} of PFBA, PFPeA, PFHxA, PFOA, P37DMOA, PFHxS and PFHpS (µ/L) in artificial groundwater spiked with PFOS (1000µg/L). Grouped after L/S ratios.

4.5 PrePFAAs

Freundlich isotherms were constructed for six precursor PFAA (prePFAA) compounds generated through the TOP assay: prePFBA, prePFPeA, prePFHxA and prePFHpA.. The plots are based on C_{eq} (µmol/L) and C_s (µmol/kg) across multiple samples (2A–6B) (figure 8).

For PFBA, the lowest C_s value was observed in sample 2B (0.22 µmol/kg), with a corresponding C_{eq} of 0.00084 µmol/L. The highest C_s occurred in sample 6A/B (1.9 µmol/kg), where the C_{eq} was also the highest for this compound at 0.063 µmol/L (6A).

PFPeA followed a similar trend. The lowest sorbed concentration was found in sample 2B (0.24 µmol/kg), with a C_{eq} of 0.0016 µmol/L. The maximum C_s value of 2.0 µmol/kg was reached in sample 6A/B, where C_{eq} was 0.0079 and 0.0064 µmol/L, respectively.

Among the tested prePFAA compounds, PFHxA showed the highest overall sorption. The lowest C_s value was 0.98 µmol/kg (2B), and the highest was 83 µmol/kg (6A). Corresponding C_{eq} values ranged from 0.0037 µmol/L (2B) to 0.0034 µmol/L (6A).

For prePFHpA, the lowest sorbed amount was found in sample 2B (0.0203 µmol/kg), with C_{eq} at 0.000118 µmol/L. The highest C_s was measured in sample 6A at 0.174 µmol/kg, with C_{eq} at 0.000263 µmol/L.

In all cases, both Cs and C_{eq} increased consistently with higher concentration levels, from the lower range samples (2A, 2B) to the highest (6A/B), which is illustrated in the Freundlich isotherms (Figure 9).

The average distribution coefficients (K_d) were also calculated for each compound based on a linear sorption model. The K_d values ranged from 329 (prePFPeA) to 635 L/kg (prePFHpA), as shown in Table 11.

To evaluate the sorption behaviour more comprehensively, both linear and Freundlich isotherm models were fitted to the data. The linear model ($C_s = K_d \cdot C_{eq}$) yielded coefficients of determination (R^2) ranging from 0.683 to 0.795 for PFBA, PFPeA, PFHxA, and PFHpA. These values indicate moderate linearity across the tested concentration ranges.

However, a better model fit was observed using the Freundlich equation ($C_s = Kf \cdot C_{eq}^n$). When plotted as log(C_s) versus log(C_{eq}), higher R^2 values were obtained, and the fitted exponents (n) ranged between 0.83 and 0.94, suggesting a slightly non-linear sorption pattern (Figure 9). The corresponding Freundlich coefficients (Kf) varied between 2.2 and 4.1 µmol/kg·(L/µmol)^n. These results show that the Freundlich model more accurately describes the sorption behaviour of the precursor compounds to the activated carbon barrier than the linear approximation.

Table 11. Partitioning coefficients (K_d) (L/kg) for prePFBA, prePFPeA, prePFHxA and prePFHpA.

	prePFBA	prePFPeA	prePFHxA	prePFHpA
K_d	459	329	407	635

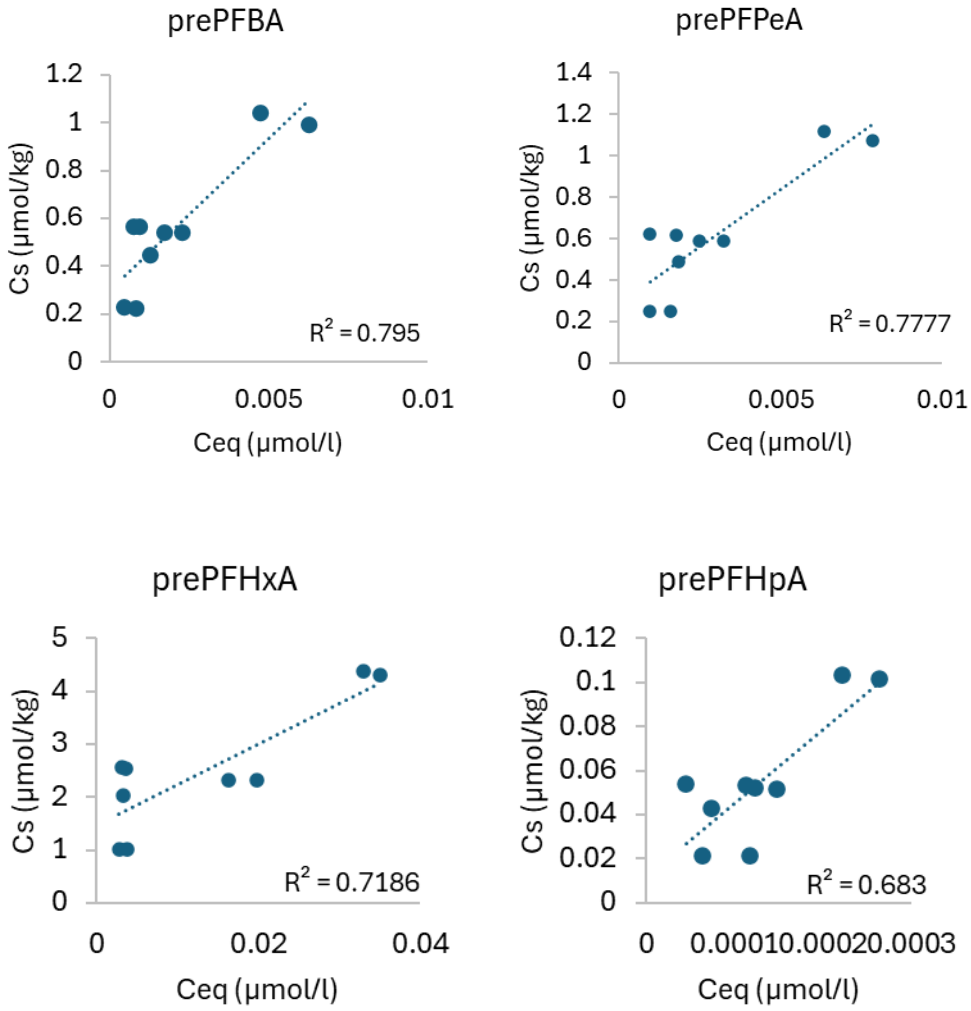

Figure 8. Freundlich sorption isotherms for pre-PFAA compounds from the TOP assay of groundwater samples. The figures show distribution between sorbed concentration in soil (C_s) (µmol/g) and PrePFAAs in aqueous phase after equilibrium (C_{eq}) (µmol/L). Each curve represents data from multiple sampling points with varying L/S ratios.

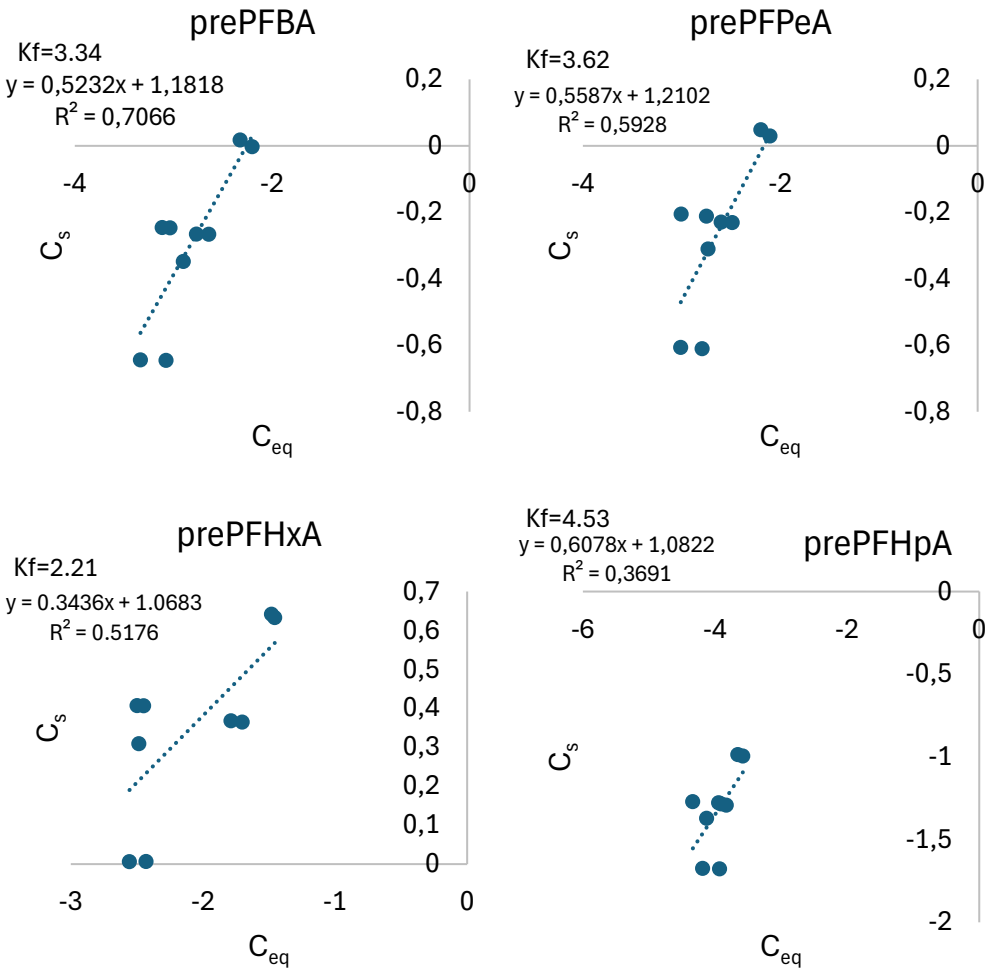

Figure 9. Freundlich isotherms for pre-PFAA compounds from the TOP assay of groundwater samples plotted as log(C_s) on y-axis and log(C_{eq}) on the x-axis. The Freundlich coefficients (Kf)is displayed in the figures.

.

4.6 pH measurements

After six days of shaking, the pH of the samples was measured. For the natural groundwater samples (1–8), pH values ranged from 6.57 to 7.10 (Table 12), with

an average of 6.86. The artificial groundwater samples (9-15) showed a slightly narrower range, from 6.64 to 6.88, with an average pH of 6.75.

Table 12. pH-values for natural groundwater system (sample 1 to 9), and for artificial groundwater (sample 13 to 15).

	pH	
Sample	A	B
1	7.01	6.98
2	7.10	7.09
3	6.88	6.66
4	6.59	6.65
5	6.92	6.83
6	6.80	6.86
7	6.95	6.88
8	6.85	6.82
9	6.84	6.88
10	6.77	6.68
11	6.73	6.80
12	6.74	6.75
13	6.75	6.68
14	6.74	6.75
15	6.73	6.64

5. Discussion

5.1 Sorption behaviour in natural groundwater

5.1.1 Retention of PFCAs and PFSAs in the natural groundwater system

Among the perfluoroalkyl sulfonic acids (PFSAs), PFOS exhibited the strongest retention in the natural groundwater system, as shown in Figure 2. Other long-chain sulfonates, such as PFHpS and PFHxS, also demonstrated substantial sorption, albeit to a slightly lesser extent. In contrast, the short-chain compound PFPeS displayed significantly weaker retention.

These observations align with well-established trends, indicating that PFAS sorption generally increases with chain length, as longer molecules exhibit greater hydrophobic interactions and stronger affinity for sorbents like activated carbon (Du et al. 2014; Milinovic et al. 2015; Sorengard et al. 2019; Sörengård et al. 2020; Niarchos et al. 2022; Bui et al. 2024). The relatively strong retention of longer-chain PFSAs further underscores the role of CAC in enhancing the sequestration of these compounds in subsurface environments.

Perfluoroalkyl carboxylic acids (PFCAs) followed a similar trend, though their overall retention was lower than that of their sulfonic acid counterparts. Longer-chain PFCAs, such as PFOA and PFHpA, exhibited moderate to strong sorption (figure 2), whereas shorter-chain acids like PFHxA and PFPeA demonstrated noticeably weaker retention. This indicates a higher leaching potential for the shorter-chain carboxylates under the tested conditions. These findings are consistent with the literature, which reports that short-chain PFAS generally exhibit higher mobility and are more prone to leaching. This pattern is particularly evident in sorption to activated carbon (AC), where short-chain PFAS rely more heavily on anion-exchange mechanisms, in contrast to long-chain PFAS that primarily interact through hydrophobic forces (Gagliano et al. 2020; Navarro et al. 2024).

When comparing PFSAs and PFCAs of similar chain lengths, sulfonic acids consistently displayed greater retention. This is likely due to differences in molecular structure and physicochemical properties, with sulfonates generally having greater molecular weight, lower water solubility, and stronger interactions with activated carbon materials (Sörengård et al. 2020). This is evident in table 8 and 9, where the retention of PFHxS clearly exceeds that of PFHxA.

The PFAS compound with the weakest overall sorption in this study was the shortest-chain carboxylate, PFBA. Its retention remained low across all tested liquid-to-solid (L/S) ratios, as shown in table 9. A slight increase in sorption was observed at higher L/S ratios, possibly due to unknown changes in solution chemistry during the experiment.

Overall, these findings highlight the combined influence of chain length and functional group on PFAS retention in CAC-amended systems. The results support the use of CAC barriers as a remediation strategy, particularly for targeting long-chain PFAS, while also emphasizing the need to consider the higher mobility of short-chain compounds in long-term risk assessments.

5.1.2 Sorption Isotherm model fit for natural groundwater

The Langmuir sorption model was generally preferred over the Freundlich model, as visual inspection of the data suggested that sorption approached saturation at higher equilibrium concentrations (C_{eq}). This behavior is characteristic of the Langmuir model, which assumes a finite sorption capacity. As shown in Figure 2, the amount of sorbed PFAS increased with increasing C_{eq} up to a certain point, after which it plateaued, indicating probable saturation of available sorption sites. In some cases, a decline in sorption was observed beyond this threshold, further supporting the appropriateness of the Langmuir model.

However, it is important to note that the Langmuir behaviour in the natural groundwater system was primarily influenced by just two samples at the highest L/S ratios, where C_{eq} was relatively elevated, which might cause uncertainties in the calculated C_s values, since these are obtained as a difference between the amount added to the system and the amount remaining in the solution after equilibration (Equation 5). At lower concentrations, the sorption trend appeared more linear. This introduces a degree of uncertainty in model selection, as the overall dataset does not exhibit a uniformly clear fit across the full concentration range. The apparent saturation behavior may therefore reflect localized conditions in those specific samples rather than a definitive system-wide trend. This uncertainty should be considered when evaluating this data set.

The saturation trend was observed for all PFAS included in the study, except for the shortest-chain compound, PFBA. This substance exhibited more scattered sorption behavior across the different L/S ratios, likely due to its higher mobility and lower affinity for the sorbent.

The potential fit to the Langmuir sorption model, where applicable, implies saturation of sorption sites in the soil. This suggests that the barrier may have a finite sorption capacity, and once saturated, it could no longer retain additional

PFAS. As a result, PFAS may begin to break through the barrier, creating a secondary source zone and potentially leading to contaminant migration downstream.

This poses a concern for long-term barrier performance. However, it remains challenging to determine exactly when saturation occurs in situ, as there is no clear indicator for breakthrough until PFAS concentrations increase on the downgradient side. Additionally, it is still uncertain whether the barrier material, such as colloidal activated carbon, can be re-injected or replenished effectively after initial saturation to restore its sorption capacity (Ross et al. 2018).

The K_{OC} values observed in this study, particularly for PFOS and PFOA, were notably higher than those commonly reported in the literature (Milinovic et al. 2015). This discrepancy is likely due to the presence of colloidal activated carbon (CAC), which was added at a low concentration but is known for its strong sorption capacity. Even small amounts of CAC can significantly enhance PFAS retention due to its high surface area and porous structure (Sörengård et al. 2020, 2022).

When compared with the results of Niarchos et al. (2023), who studied PFAS sorption to CAC alone, the K_{OC} values observed in this study were in several cases higher. Notably, compounds such as PFHpA, PFHxS, and PFOS exhibited substantially higher retention, suggesting that the combination of CAC and natural soil components, particularly soil organic matter may enhance PFAS sorption compared to CAC in isolation. One possible explanation is that the heterogeneity of the amended system offers a broader range of sorption mechanisms, including hydrophobic interactions with organic matter and electrostatic interactions with mineral surfaces. Furthermore, CAC may behave differently when embedded in soil, possibly due to altered surface accessibility or changes in the surrounding microenvironment. These findings highlight that while CAC is a highly effective sorbent, its performance can be further influenced, positively or negatively by the surrounding matrix, which should be considered when designing in situ remediation systems.

In contrast to natural soils, K_{OC} values are generally reported to be around 700 L/kg for PFOS (Milinovic et al. 2015), which is substantially lower than the much higher K_{OC} value observed in this study for the CAC-amended soil (approximately 1.9E0+5 L/kg). This marked increase in sorption capacity highlights the significant effect of CAC amendment in enhancing PFAS retention in the soil matrix.

5.1.3 Comparison with untreated soil

The comparison with the untreated reference soil confirms that the addition of colloidal activated carbon (CAC) substantially increases the sorption capacity for PFAS. In the absence of CAC, all tested compounds showed considerably lower Kd and KOC values, indicating weaker sorption to the soil matrix (Table 10). This is consistent with previous research showing that PFAS sorption in natural soils is typically low unless amended with sorbent materials (Navarro et al. 2023). The improvement in sorption with CAC is particularly relevant for long-chain PFAS like PFHpS and PFOS, which exhibited the most pronounced increase in both Kd and KOC. The enhanced retention is likely due to the high surface area and hydrophobic properties provided by the CAC.

It is important to highlight, however, that Kd values for the reference samples (8A/B) (table 10) without CAC are associated with substantial analytical uncertainty. Because the adsorbed concentration is calculated as the difference between two relatively large values (initial and final aqueous concentrations), small analytical deviations can lead to large variations in calculated Kd. This makes accurate determination of Kd for weakly sorbing substances like PFAS especially challenging. For instance, although the data suggest minor differences in Kd between PFBA, PFOA, and PFHpS, these results must be interpreted with caution. In reality, all Kd values for these compounds in unamended soils are likely close to zero, particularly for short-chain PFAS such as PFBA, which are known to exhibit very weak soil interactions. This also aligns with established PFAS behavior, where sorption strength increases with chain length and functional group hydrophobicity, PFOS and PFHpS being more strongly retained than PFBA.

These limitations underscore the need for careful interpretation of Kd data from low-sorption matrices and support the use of engineered sorbents like CAC in in-situ remediation strategies. The most reliable Kd values in this study were obtained at the lowest L/S ratio, where the concentration gradient between the solid and aqueous phases was greatest and experimental uncertainty minimized. These results emphasize the critical role of sorbent selection in designing effective in-situ barriers for PFAS retention.

5.2 Sorption behaviour isolated PFOS system

5.2.1 Sorption Isotherm for artificial groundwater system

Although the system was designed as a single-solute PFOS system, post-equilibration analysis revealed the presence of several additional PFAS compounds. This was likely due to the PFOS standard containing impurities, as the reported purity was ≥98%. Thus, other PFAS particularly long-chain sulfonates and short-chain carboxylic acids may have been present in small amounts and contributed to the observed concentrations. These co-contaminants were not added intentionally and their presence introduces some uncertainty in interpreting this system as purely PFOS-based.The calculated Kd value for this system was 264 L/kg, aligning with values reported in the literature (Niarchos et al. 2023). The sorption followed a linear trend, indicating that within the tested concentration range, no saturation of sorption sites occurred. This linear behavior suggests that PFOS partitioned into the solid phase proportionally to its aqueous concentration, and that the sorption capacity of the CAC-amended barrier was not yet exceeded. Such behavior is commonly observed in systems with low PFAS concentrations, homogeneous sorbents, and minimal interference from other compounds, and aligns with previous batch studies reporting similar linear sorption trends for PFOS (Milinovic et al. 2015).

When comparing isolated PFOS sorption under single-solute conditions, the K_{OC} value observed in this study was higher than that reported by Niarchos et al. for a comparable single-solute system. This indicates that, although CAC is an effective sorbent on its own, the presence of soil organic matter and the absence of competition from other PFAS may contribute to stronger retention of PFOS in the amended system.

5.2.2 Comparison between artificial groundwater system and natural groundwater system

When comparing this behavior to PFOS sorption in the natural groundwater system, a nonlinear, Langmuir isotherm was observed. At low C_{eq} and C_s values, the relationship appeared roughly linear, but at higher concentrations (in two samples at the highest L/S ratios), a levelling off was seen. This suggests the onset of sorption site saturation or possibly competition with other PFAS. However, since only two high-L/S samples showed this behavior, the trend is not definitive. It is therefore uncertain whether this pattern reflects a meaningful environmental process, or a context-specific outcome limited to this batch setup.

This highlights a limitation in extrapolating Langmuir-type behavior to field conditions based on limited high-concentration data points. While the natural system showed a higher K_d of 402 L/kg, indicating overall stronger retention of PFOS, it is unclear whether this translates into higher affinity or simply reflects complex matrix interactions.

The contrasting sorption profiles between the artificial and natural groundwater systems underscore the influence of PFAS competition and matrix effects on sorption processes. In the artificial system, PFOS sorption followed a clear linear uptake pattern. However, due to the presence of co-contaminants likely introduced through the PFOS standard, some interference may still have occurred, particularly at low concentrations. Nevertheless, the absence of naturally occurring background PFAS and the dominance of PFOS allowed a clearer interpretation of single-compound sorption behavior compared to the natural groundwater system.

5.2.3 Displacement of native PFAS from soil

The batch tests using artificial groundwater spiked with PFOS revealed unexpectedly high concentrations of additional PFAS compounds in the aqueous phase after equilibrium. While small background levels of certain PFAS were known to exist in the soil prior to testing, calculations of desorbed mass consistently exceeded 100% for all detected substances. This indicates that the soil alone could not be the source of the PFAS measured in the water phase.

A likely explanation is the presence of co-contaminants in the PFOS standard used for spiking. Although the standard was assumed to be pure PFOS, the manufacturer reported a purity of ≥98%. This means that more than 2% of the material may have consisted of other PFAS compounds. Given the analytical sensitivity of the method used and the high spiking concentrations, even small amounts of impurities could result in detectable levels of other PFAS in the solution, especially long-chain compounds like PFHpS and PFCAs such as PFPeA or PFHxA.

The results underscore a critical limitation in assuming purity in commercial PFAS standards. In this case, the unexpected detection of multiple PFAS suggests that the elevated concentrations observed cannot be solely attributed to desorption from the soil matrix, but rather point toward the standard as the primary source. This finding highlights the importance of verifying the chemical composition of standard solutions, particularly when working with trace-level analyses and complex environmental matrices.

Future studies should consider pre-screening standard solutions to identify and account for potential impurities. Additionally, a background test of the spiking

solution alone (without soil) could help differentiate between contributions from the soil and the chemical standard.

5.3 Precursor compounds

5.3.1 Sorption of prePFAAs to Colloidal Activated Carbon barrier

Transformation of precursor compounds into perfluoroalkyl acids (PFAAs) through the TOP assay could clearly be seen in the groundwater samples. Freundlich isotherms were made for four prePFAAs generated from precursors, and these isotherms show increasing sorption (C_s) with increasing equilibrium concentration (C_{eq}) across all samples (Figure 8). This suggests that, although precursor-derived PFAAs are present at relatively low concentrations, they still can have measurable interactions with the CAC-amended soil.

Among the tested compounds, sorption strength varied; prePFHxA exhibited the highest sorbed concentrations and the greatest liquid-to-solid partitioning, as reflected in its Freundlich curve (Figure 8). This indicates that certain precursor-derived PFAAs may have a greater affinity for CAC than others, potentially due to optimal chain length and hydrophobicity for interaction with the sorbent.

Precursor compounds leading to short-chain PFAAs, such as prePFBA and prePFPeA, showed moderate sorption capacities. Despite ultimately degrading into short-chain PFAS, these precursors are high molecular weight compounds that exhibit sorption behavior more similar to long-chain PFAS like PFOS. Their relatively strong affinity for CAC is likely due to their larger molecular size and greater hydrophobicity (Ross et al. 2018; Sörengård et al. 2020; Liu et al. 2022).

When comparing the K_d values of these precursor compounds to those reported for PFOS in natural groundwater systems, it is notable that most of the precursor K_d values fall within a similar range as PFOS, a long-chained PFSA known for its strong affinity to solid phases. This suggests that many precursor-derived compounds may sorb to the CAC barrier with comparable strength, supporting their potential contribution to overall PFAS retention. However, the variation in K_d among the precursors also highlights that sorption is compound-specific and influenced by molecular characteristics.

There are limitations to this interpretation. Sorption experiments were conducted under controlled laboratory conditions, which may not fully represent complex field environments where multiple competing processes and matrix effects influence PFAS behaviour. Furthermore, while the Freundlich model captured non-linear sorption trends more accurately than the linear model, the K_d

values calculated under linear assumptions are still useful as comparative metrics, especially when discussing partitioning relative to known PFAS like PFOS.

In conclusion, these results demonstrate that precursor compounds generated through oxidative transformation have a high affinity to bind to the CAC barrier, often in the same range as PFOS. This finding underlines the importance of including precursor-derived PFAS in sorption and risk assessments, as they may contribute significantly to long-term retention and persistence in remediation systems. It also emphasizes the need for comprehensive evaluation of PFAS mixtures rather than focusing solely on terminal perfluoroalkyl acids.

5.4 pH Conditions and Their Potential Influence

The average pH of the natural groundwater was 6.86, while the artificial groundwater had an average pH of 6.75 (table 12). This means the artificial groundwater was only 0.11 units lower in pH than the natural groundwater, and it is also close to the target pH of 7.0 that was set prior to the batch tests. All pH values were measured after equilibrium had been reached.

However, a limitation in the procedure was that the pH of the natural groundwater was not measured immediately after preparation. As a result, the measured pH values may have been influenced by interactions between the soil and the solution during the batch test period. Both the soil matrix and the PFAS compounds released from the soil could potentially affect the pH. For instance, sorption or desorption processes, ionic exchange, or the presence of acidic or basic functional groups on the soil particles could alter the pH of the solution over time.

Therefore, it cannot be ruled out that the natural groundwater had a pH closer to 7.0 prior to contact with the soil, and the observed values may not fully reflect the original state of the solution.

5.5 Limitations

For the artificial groundwater used in the PFOS system, a blank sample should have been submitted for PFAS analysis prior to the batch shaking tests to assess any background contamination. Since several PFAS compounds (other than PFOS) were detected in the aqueous phase after the tests, it cannot be ruled out that some of these may have been present in the solution from the beginning. Although the observed concentrations were relatively high and unlikely to

originate from the Milli-Q water alone, the lack of an initial blank makes it difficult to confirm their exact source.

5.6 Implications for In Situ Applications

While this study provides valuable insight into the sorption behavior of PFAS to CAC-amended soil, translating these findings into in situ barrier systems requires consideration of additional factors. In field-scale applications, the injected CAC interacts with a dynamic subsurface environment where groundwater flow, heterogeneity in soil properties, and variable contact times influence barrier performance. The batch experiments presented here simulate increasing cumulative loading through higher L/S ratios, which may be used as a proxy for long-term exposure under natural site conditions. The observed non-linear sorption behavior and saturation effects at high L/S ratios indicate that CAC barriers may have limited retention capacity over time, especially in complex PFAS mixtures. This underlines the importance of accounting for both competition between PFAS and non-linear sorption when modeling breakthrough and estimating barrier longevity under site-relevant conditions. Future modeling and pilot-scale testing could incorporate these factors to improve predictive accuracy for full-scale in situ applications.

5.7 Conclusion

This study demonstrates that PFAS sorption to colloidal activated carbon (CAC)-amended soil is influenced by both the chemical composition of the groundwater and the liquid-to-solid (L/S) ratio of the system. Among the PFAS compounds studied, long-chain substances, especially sulfonic acids like PFOS exhibited the highest retention, while short-chain showed weaker sorption. Notably precursor-derived PFAS exhibited sorption comparable to PFOS. Sorption behavior followed Langmuir trends in the natural groundwater system, suggesting a finite sorption capacity and potential for saturation, particularly under higher L/S ratios. In contrast, PFOS sorption in the artificial system was linear, indicating a lack of saturation and absence of competition.

The comparison of natural and artificial systems reveals that matrix complexity plays a critical role in sorption dynamics. In the natural groundwater, co-occurring PFAS likely competed for sorption sites, leading to nonlinear behavior and possible displacement effects. In the artificial system, PFOS sorption was uninfluenced by such interactions, underscoring the importance of using representative groundwater matrices when evaluating remediation materials.

Precursor-derived PFAS (prePFAAs), although present at lower concentrations than PFOS, demonstrated strong sorption to CAC-amended soil, with some compounds showing partitioning behavior comparable to PFOS. This finding reinforces the necessity of accounting for precursors when assessing long-term barrier performance.

Overall, the results support the application of CAC-based barriers for in situ remediation of PFAS, particularly for long-chain compounds. However, the potential for saturation, competition, and precursor transformation underlines the importance of comprehensive monitoring and adaptive management in field deployments.

5.8 Future recommendations

Overall, these findings suggest that CAC-amended barriers are promising for in-situ PFAS remediation, particularly for long-chain compounds. However, their effectiveness against short-chain PFAS and precursor transformation products remains a challenge. Future work should focus on long-term monitoring, potential barrier rejuvenation (e.g., re-injection), and comprehensive analysis of precursor dynamics to improve risk assessments and barrier design strategies.

The present study offers valuable insights into PFAS retention in CAC-amended soil under controlled conditions, but several areas warrant further investigation to enhance the applicability of these findings to real-world scenarios.

- Field validation: Future studies should examine CAC barrier performance under field conditions, where dynamic hydraulic flow, natural heterogeneity, and aging of the barrier material may affect long-term sorption behavior.
- Long-term saturation and breakthrough: The Langmuir-type sorption observed at higher L/S ratios suggests that sorption sites may become saturated over time. Long-duration column tests or pilot-scale field installations could help estimate the timeline and threshold for breakthrough events.
- Regeneration or replenishment of CAC barriers: As saturation appears likely under extended loading, research should investigate whether CAC barriers can be re-injected, rejuvenated, or replaced in situ without disturbing the surrounding environment.
- Precursor dynamics and transformation: Since precursor-derived PFAS sorbed to the CAC in measurable amounts, it is important to further explore

the transformation kinetics, sorption behavior, and persistence of these compounds, especially under oxidative or reducing subsurface conditions.

- Effect of variable groundwater chemistry: Additional work should assess how parameters such as ionic strength, dissolved organic matter, competing ions, and pH influence sorption dynamics in CAC barriers.

Collectively, these future directions can support the development of robust, field-ready strategies for using CAC in sustainable PFAS remediation efforts.

6. References

Ahrens, L. & Bundschuh, M. (2014). Fate and effects of poly- and perfluoroalkyl substances in the aquatic environment: A review. *Environmental Toxicology and Chemistry*, 33 (9), 1921–1929. https://doi.org/10.1002/etc.2663

Ahrens, L., Norström, K., Viktor, T., Cousins, A.P. & Josefsson, S. (2015). Stockholm Arlanda Airport as a source of per- and polyfluoroalkyl substances to water, sediment and fish. *Chemosphere*, 129, 33–38. https://doi.org/10.1016/j.chemosphere.2014.03.136

Ahrens, L., Taniyasu, S., Yeung, L.W.Y., Yamashita, N., Lam, P.K.S. & Ebinghaus, R. (2010). Distribution of polyfluoroalkyl compounds in water, suspended particulate matter and sediment from Tokyo Bay, Japan. *Chemosphere*, 79 (3), 266–272. https://doi.org/10.1016/j.chemosphere.2010.01.045

Buck, R.C., Franklin, J., Berger, U., Conder, J.M., Cousins, I.T., de Voogt, P., Jensen, A.A., Kannan, K., Mabury, S.A. & van Leeuwen, S.P. (2011). Perfluoroalkyl and polyfluoroalkyl substances in the environment: Terminology, classification, and origins. *Integrated Environmental Assessment and Management*, 7 (4), 513–541. https://doi.org/10.1002/ieam.258

Bui, T.H., Zuverza-Mena, N., Dimkpa, C.O., Nason, S.L., Thomas, S. & White, J.C. (2024). PFAS remediation in soil: An evaluation of carbon-based materials for contaminant sequestration. *Environmental Pollution*, 344, 123335. https://doi.org/10.1016/j.envpol.2024.123335

Du, Z., Deng, S., Bei, Y., Huang, Q., Wang, B., Huang, J. & Yu, G. (2014). Adsorption behavior and mechanism of perfluorinated compounds on various adsorbents—A review. *Journal of Hazardous Materials*, 274, 443–454. https://doi.org/10.1016/j.jhazmat.2014.04.038

Essington, M.E. (2004). *Soil and water chemistry: an integrative approach*. https://www.researchgate.net/publication/311477742_Soil_and_water_chemistry_an_integrative_approach [2025-02-05]

Eurofins Scientific (n.d.). *Eurofins Scientific*. https://www.eurofins.se/ [2025-06-02]

Evich, M.G., Davis, M.J.B., McCord, J.P., Acrey, B., Awkerman, J.A., Knappe, D.R.U., Lindstrom, A.B., Speth, T.F., Tebes-Stevens, C., Strynar, M.J., Wang, Z., Weber, E.J., Henderson, W.M. & Washington, J.W. (2022). Per- and polyfluoroalkyl substances in the environment. *Science*, 375 (6580). https://doi.org/10.1126/science.abg9065

Gagliano, E., Sgroi, M., Falciglia, P.P., Vagliasindi, F.G.A. & Roccaro, P. (2020). Removal of poly- and perfluoroalkyl substances (PFAS) from water by adsorption: Role of PFAS chain length, effect of organic matter and challenges in adsorbent regeneration. *Water Research*, 171, 115381. https://doi.org/10.1016/j.watres.2019.115381

Gyllenhammar, I., Berger, U., Sundström, M., McCleaf, P., Eurén, K., Eriksson, S., Ahlgren, S., Lignell, S., Aune, M., Kotova, N. & Glynn, A. (2015). Influence of contaminated drinking water on perfluoroalkyl acid levels in human serum – A case study from Uppsala, Sweden. *Environmental Research*, 140, 673–683. https://doi.org/10.1016/j.envres.2015.05.019

Hansson, K., Cousins, A.P., Norström, K., Graae, L. & Stenmarck, Å. (2016). *Sammanställning av befintlig kunskap om föroreningskällor till PFAS-ämnen i svensk miljö*. (C182). https://ivl.diva-portal.org/smash/get/diva2:1549779/FULLTEXT01.pdf [2025-01-30]

Kärrman, A., Wang, T., Kallenborn, R., Langseter, A.M., Grønhovd, S.M., Ræder, E.M., Lyche, J.L., Yeung, L., Chen, F., Eriksson, U., Aro, R. & Fredriksson, F. (2019). *PFASs in the Nordic environment: Screening of Poly- and Perfluoroalkyl Substances (PFASs) and Extractable Organic Fluorine (EOF) in the Nordic Environment*. Nordic Council of Ministers.

Koch, A., Jonsson, M., Yeung, L.W.Y., Kärrman, A., Ahrens, L., Ekblad, A. & Wang, T. (2020). Per- and Polyfluoroalkyl-Contaminated Freshwater Impacts Adjacent Riparian Food Webs. *Environmental Science & Technology*, 54 (19), 11951–11960. https://doi.org/10.1021/acs.est.0c01640

Kookana, R.S., Navarro, D.A., Kabiri, S. & McLaughlin, M.J. (2023). Key properties governing sorption–desorption behaviour of poly- and perfluoroalkyl substances in saturated and unsaturated soils: a review. https://www.researchgate.net/publication/366344294_Key_properties_governing_sorption-desorption_behaviour_of_poly-_and_perfluoroalkyl_substances_in_saturated_and_unsaturated_soils_a_review [2025-03-05]

Lange, F.T., Freeling, F. & Göckener, B. (2024). Persulfate-based total oxidizable precursor (TOP) assay approaches for advanced PFAS assessment in the environment – A review. *Trends in Environmental Analytical Chemistry*, 44, e00242. https://doi.org/10.1016/j.teac.2024.e00242

Leung, S.C.E., Wanninayake, D., Chen, D., Nguyen, N.-T. & Li, Q. (2023). Physicochemical properties and interactions of perfluoroalkyl substances (PFAS) - Challenges and opportunities in sensing and remediation. *Science of The Total Environment*, 905, 166764. https://doi.org/10.1016/j.scitotenv.2023.166764

Liu, C.J., Murray, C.C., Marshall, R.E., Strathmann, T.J. & Bellona, C. (2022). Removal of per- and polyfluoroalkyl substances from contaminated groundwater by granular activated carbon and anion exchange resins: a pilot-scale comparative assessment. *Environmental Science: Water Research & Technology*, 8 (10), 2245–2253. https://doi.org/10.1039/D2EW00080F

Livsmedelsverket (2023). *PFAS och andra miljögifter i dricksvatten och livsmedel - kontroll*. *Livsmedelverket*. https://www.livsmedelsverket.se/foretagande-regler-kontroll/dricksvattenproduktion/kontroll-pfas-miljogifter-dricksvatten-egenfangad-fisk [2023-12-11]

Milinovic, J., Lacorte, S., Vidal, M. & Rigol, A. (2015). Sorption behaviour of perfluoroalkyl substances in soils. *Science of The Total Environment*, 511, 63–71. https://doi.org/10.1016/j.scitotenv.2014.12.017

Mussabek, D., Söderman, A., Imura, T., M.Persson, K., Nakagawa, K., Ahrens, L. & Berndtsson, R. (2023). PFAS in the Drinking Water Source: Analysis of the Contamination Levels, Origin and Emission Rates. https://doi.org/10.3390/w1510137

Navarro, D.A., Kabiri, S.S., Bowles, K., Knight, E.R., Braeunig, J., Srivastava, P., Boxall, N.J., Douglas, G., Mueller, J., McLaughlin, M.J., Williams, M. & Kookana, R.S. (2024). Review on Methods for Assessing and Predicting Leaching of PFAS from Solid Matrices. *Current Pollution Reports*, 10 (4), 628–647. https://doi.org/10.1007/s40726-024-00326-6

Niarchos, G., Ahrens, L., Kleja, D.B. & Fagerlund, F. (2022). Per- and polyfluoroalkyl substance (PFAS) retention by colloidal activated carbon (CAC) using dynamic column experiments. *Environmental Pollution*, 308, 119667. https://doi.org/10.1016/j.envpol.2022.119667

Niarchos, G., Georgii, L., Ahrens, L., Kleja, D.B. & Fagerlund, F. (2023). A systematic study of the competitive sorption of per- and polyfluoroalkyl

substances (PFAS) on colloidal activated carbon. *Ecotoxicology and Environmental Safety*, 264, 115408. https://doi.org/10.1016/j.ecoenv.2023.115408
OECD (2013). *Synthesis paper on per and polyfluorinated chemicals | OECD*. https://www.oecd.org/en/publications/synthesis-paper-on-per-and-polyfluorinated-chemicals_0bc75123-en.html [2025-01-27]
OECD (2018). *Summary report on the new comprehensive global database of Per- and Polyfluoroalkyl Substances (PFASs)*. *OECD*. https://www.oecd.org/en/publications/summary-report-on-the-new-comprehensive-global-database-of-per-and-polyfluoroalkyl-substances-pfass_1a14ad6c-en.html [2025-01-30]
Ross, I., McDonough, J., Miles, J., Storch, P., Thelakkat Kochunarayanan, P., Kalve, E., Hurst, J., S. Dasgupta, S. & Burdick, J. (2018). A review of emerging technologies for remediation of PFASs. *Remediation Journal*, 28 (2), 101–126. https://doi.org/10.1002/rem.21553
Sadia, M., Beut, L.B., Pranić, M., Wezel, A.P. van & Laak, T.L. ter (2024). Sorption of per- and poly-fluoroalkyl substances and their precursors on activated carbon under realistic drinking water conditions: Insights into sorbent variability and PFAS structural effects. *Heliyon*, 10 (3), e25130. https://doi.org/10.1016/j.heliyon.2024.e25130
SGI (2025). *Stabilisering av PFAS till sorbent i jord*. http://www.sgi.se/vara-expertomraden/fororenade-omraden/fororenad-mark-vatten-och-sediment/pfas---hogfluorerande-amnen/uppdrag-om-forskning-och-okad-kunskap-om-pfas-fororenade-omraden/stabilisering-av-pfas-till-sorbent-i-jord [2025-06-06]
Sörengård, M., Bergström, S., McCleaf, P., Wiberg, K. & Ahrens, L. (2022). Long-distance transport of per- and polyfluoroalkyl substances (PFAS) in a Swedish drinking water aquifer. *Environmental Pollution*, 311, 119981. https://doi.org/10.1016/j.envpol.2022.119981
Sorengard, M., Kleja, D.B. & Ahrens, L. (2019). Stabilization of per- and polyfluoroalkyl substances (PFASs) with colloidal activated carbon (PlumeStop®) as a function of soil clay and organic matter content. *Journal of Environmental Management*, 249, 109345. https://doi.org/10.1016/j.jenvman.2019.109345
Sörengård, M., Östblom, E., Köhler, S. & Ahrens, L. (2020). Adsorption behavior of per- and polyfluoralkyl substances (PFASs) to 44 inorganic and organic sorbents and use of dyes as proxies for PFAS sorption. *Journal of Environmental Chemical Engineering*, 8 (3), 103744. https://doi.org/10.1016/j.jece.2020.103744
Swedish Chemicals Agency (2025). *PFAS*. *PFAS*. [text]. https://www.kemi.se/en/chemical-substances-and-materials/pfas [2025-01-23]

Popular science summary

6.1 PFAS in Soil and Water: Can Colloidal Activated Carbon Particles Help Stop the Spread?

PFAS (per- and polyfluoroalkyl substances) are synthetic chemicals used in products like firefighting foam, non-stick coatings, and water-repellent fabrics. They are often called “forever chemicals” because they don’t easily break down in the environment. Over time, PFAS can spread into groundwater and pose risks to both people and ecosystems.

One possible solution is to install barriers in the ground that trap PFAS before they move with the water. This study explored whether adding colloidal activated carbon (CAC), very small particles of carbon, into the soil could help stop PFAS from spreading. The tests were done in a laboratory using both natural and artificial groundwater, with different amounts of water and soil to simulate different conditions.

The results showed that long-chain PFAS, like PFOS, were effectively trapped by CAC, while short-chain PFAS, like PFBA, were much harder to stop. The study also found that some PFAS precursors, chemicals that can transform into PFAS, through transformation using a method called the Total Oxidizable Precursor (TOP) assay. Could also bind to the carbon particles in the barrier.

The research highlights that CAC can be a useful material in in-situ barriers to reduce PFAS movement, especially for the more harmful long-chain compounds. However, it also shows that short-chain PFAS and precursors remain a challenge and may pass through the barrier more easily. Additionally, the effectiveness of these barriers can change depending on the real chemistry of the local groundwater, which influences how well PFAS are retained.

In summary, this study supports using CAC to slow down the spread of PFAS in contaminated soil and groundwater. But to ensure these barriers work in the long term, especially in the field, they must be tested under realistic conditions that reflect the complexity of natural groundwater.

Appendix 1

Appendix 1 contains a ZIP file with raw data used as the basis for the results and interpretations presented in this thesis. The folder includes original analysis files from Eurofins and soil characterization data. These data form the foundation for the evaluation of PFAS concentrations and sorption behavior in both water and soil systems.

The following files are included:

- Eurofins data – Groundwater analysis
- Eurofins data – Samples 1–3
- Eurofins data – Samples 2–4
- Eurofins data – Samples 5–8
- Eurofins data – Samples 7A
- Soil data

These files have been processed and interpreted in the main body of the thesis. If the appendix is not included in the published version, the data can be made available upon request.

Publishing and archiving

Approved students' theses at SLU can be published online. As a student you own the copyright to your work and in such cases, you need to approve the publication. In connection with your approval of publication, SLU will process your personal data (name) to make the work searchable on the internet. You can revoke your consent at any time by contacting the library.

Even if you choose not to publish the work or if you revoke your approval, the thesis will be archived digitally according to archive legislation.

You will find links to SLU's publication agreement and SLU's processing of personal data and your rights on this page:

- https://libanswers.slu.se/en/faq/228318

☒ YES, I, Frida Lundell, have read and agree to the agreement for publication and the personal data processing that takes place in connection with this.

☐ NO, I/we do not give my/our permission to publish the full text of this work. However, the work will be uploaded for archiving and the metadata and summary will be visible and searchable.